UNIVERSITY OF CALIFORNIA SAN DIEGO

Wildfires, Floods, and Climate Variability

A dissertation submitted in partial satisfaction of the requirements
for the degree of Doctor of Philosophy

in

Economics

by

Thomas William Corringham

Committee in charge:

Richard Carson, Chair
Daniel Cayan, Co-Chair
Judson Boomhower
Mark Jacobsen
Craig McIntosh

2018

The Dissertation of Thomas William Corringham is approved, and it is acceptable in quality and form for publication on microfilm and electronically:

_____

_____

_____

_____

Co-Chair

_____

Chair

University of California San Diego

2018

DEDICATION

To my parents.

TABLE OF CONTENTS

LIST OF ABBREVIATIONS

AR	Atmospheric River
BEA	Bureau of Economic Analysis
BLM	Bureau of Land Management
CCA	Canonical Correlation Analysis
CEFA	Program for Climate, Ecosystem, and Fire Applications
ENSO	El Niño Southern Oscillation
EOF	Empirical Orthogonal Function
ESA	Endangered Species Act
FWS	Fish and Wildlife Service
GACC	Geographic Area Coordination Centers
GDP	Gross Domestic Product
GIS	Geographic Information System
IVT	Integrated Vapor Transport
IWV	Integrated Water Vapor
MEI	Multivariate ENSO Index
NICC	National Interagency Coordinating Center
NFIC	National Interagency Fire Center
NFIP	National Flood Insurance Program
NOAA	National Oceanographic and Atmospheric Administration
NPS	National Parks Service
NWCG	National Wildfire Coordinating Group
NWS	National Weather Service
ONDJFM	October, November, December, January, February, March

PC	Principal Component
PCA	Principal Components Analysis
PDO	Pacific Decadal Oscillation
RISA	Regional Integrated Science and Assessment
SIO	Scripps Institution of Oceanography
SST	Sea Surface Temperature
USDOI	US Department of the Interior
VIC	Variable Infiltration Capacity

LIST OF FIGURES

LIST OF TABLES

ACKNOWLEDGEMENTS

I would like to acknowledge my chair Richard Carson, my co-chair Dan Cayan, my committee members, and my co-authors, and an NSF IGERT fellowship for funding part of my graduate studies.

Chapter 1, in full, is a reprint of the material as it appears in Exploring Use of Climate Information in Wildland Fire Management: A Decision Calendar Study, 2008. Corringham, Thomas W.; Westerling, Anthony L.; Morehouse, Barbara J., Journal of Forestry, 106(2): 71-77. Tom Corringham was the primary investigator and author of this paper.

Chapter 2, in full, is currently being prepared for submission for publication of the material. Corringham, Thomas W.; Cayan, Daniel R. Tom Corringham was the primary investigator and author of this material.

Chapter 3, in full, is currently being prepared for submission for publication of the material. Corringham, Thomas W.; Gershunov, Alexander; Cayan, Daniel R. Tom Corringham was the primary investigator and author of this material.

VITA

EDUCATION

2018 Doctor of Philosophy, Economics, University of California San Diego

2010 MA (Oxon.), Philosophy, Politics and Economics, University of Oxford

2000 BA (Hons.), Philosophy, Politics and Economics, University of Oxford

AWARDS

NSF IGERT Fellow, Scripps Institution of Oceanography (SIO) 2003 – 2004

National Merit Scholar 1996 – 2000

EMPLOYMENT

Graduate Student Researcher: SIO Climate Research Division, 2002 – 2009

Lecturer: UCSD Department of Economics, 2007 – 2008

Teaching Assistant: UCSD Department of Economics, 2002 – 2008

FIELDS OF STUDY

Major Fields: Environmental Economics and Applied Climatology

ABSTRACT OF THE DISSERTATION

Wildfires, Floods, and Climate Variability

by

Thomas William Corringham

Doctor of Philosophy in Economics

University of California San Diego 2018

Richard Carson, Chair
Daniel Cayan, Co-Chair

The first chapter surveys fire and fuels managers at local, regional, and national levels. Survey results in the form of fire managers' decision calendars show how climate information needs vary seasonally, over space, and through the organizational network. The study identifies opportunities to use climate information in fire management, including seasonal to inter-annual climate forecasts at all organizational levels, to improve the targeting of fuels treatments and prescribed burns, the positioning and movement of initial attack resources, and staffing and budgeting decisions.

The second chapter analyzes National Flood Insurance Program (NFIP) data to quantify the economic impacts of flooding across the western United States from 1978 to 2007. The study compares National Flood Insurance Program data to National Weather Service measures of total damages, and presents a spatial and temporal analysis of daily claims and loss data over this period. The NFIP data reveals that a small number winter-season extreme hydrologic events, covering wide spatial areas, are responsible for a large proportion of total losses. In coastal southern California and across the southwest, El Niño conditions have had a strong effect in producing more frequent and higher magnitudes of insured losses while La Niña conditions significantly reduce both the frequency and magnitude losses. In the Pacific Northwest, the opposite pattern appears, though the effect is somewhat weaker, and less spatially coherent.

The third chapter quantifies the economic impacts of flooding due to atmospheric river (AR) events in the western United States from 1978 to 2007, using NFIP claims and loss data. The study confirms that AR-related flood events cause significant economic damages and form the primary source of insurance claims and insured flood losses in the western coastal states. It provides spatial and temporal characterizations of damages as a function of integrated vapor transport (IVT) and antecedent hydrologic conditions.

As the magnitude and frequency of wildfire and flood events change in response to anthropogenic climate change, and as economic and demographic contributions to vulnerability increase over time, public policy must adapt to respond. The results in these papers may be used to inform policies to mitigate losses and respond to future disaster scenarios, and may be of interest to policy makers and applied climate researchers alike.

Exploring Use of Climate Information in Wildland Fire Management: A Decision Calendar Study

Thomas W. Corringham, Anthony L. Westerling, and Barbara J. Morehouse

ABSTRACT

We conducted surveys of fire and fuels managers at local, regional, and national levels to gain insights into decision processes and information flows in wildfire management. Survey results in the form of fire managers' decision calendars show how climate information needs vary seasonally, over space, and through the organizational network, and help determine optimal points for introducing climate information and forecasts into decision processes. We identified opportunities to use climate information in fire management, including seasonal to interannual climate forecasts at all organizational levels, to improve the targeting of fuels treatments and prescribed burns, the positioning and movement of initial attack resources, and staffing and budgeting decisions. Longer-term (5–10 years) outlooks also could be useful at the national level in setting budget and research priorities. We discuss these opportunities and examine the kinds of organizational changes that could facilitate effective use of existing climate information and climate forecast capabilities.

Keywords: climate, forecasts, western United States, wildfire management

Devastating wildfires flaming across large expanses of the United States in recent years have galvanized politicians, fire managers, and ordinary citizens alike in an effort to understand the processes driving catastrophic fire and to develop ways to anticipate when and where severe fire is likely to occur over time and space. Properly designed and used scientific knowledge and information, including climate information and forecasts, can contribute to better fire prediction and management. An essential first step in this process involves identifying optimal points in the decision networks of agencies charged with wildland fire management where such information may be inserted into decision processes. This, in turn, requires understanding the annual cycle of decisionmaking within the multiagency wildland fire management structure. The study reported here developed monthly decision calendars for National Forest Service and Park Service management units in California and the Southwest. These were used to identify points where scientific knowledge about climate–fire interactions are or may be productively introduced and to discuss the potential value of such information in strategic fire planning processes.

Background

Since the 1970s there has been a dramatic rise in the area burned by wildfires in the western United States. The average annual reported area burned in forest wildfires

Received July 23, 2007; accepted February 7, 2008.

Thomas W. Corringham (tcorringham@ucsd.edu) is graduate student, Department of Economics, University of California, San Diego, 9500 Gilman Drive, Mail Stop 0534, La Jolla, CA 92093-0534. Anthony L. Westerling (awesterling@ucmerced.edu) is assistant professor of environmental engineering and geography, Sierra Nevada Research Institute, University of California, Merced, CA 95344. Barbara J. Morehouse (morehoub@u.arizona.edu) is deputy director, Institute for the Study of Planet Earth, University of Arizona, Tucson, AZ 85721. *The authors thank N. Kada, T. Wordell, R. Ochoa, T. Brown, and survey respondents for their assistance. All errors and omissions are ours alone. This work was supported by a grant from the National Oceanographic and Atmospheric Administration's Office of Global Programs via the Climate Assessment for the Southwest.*

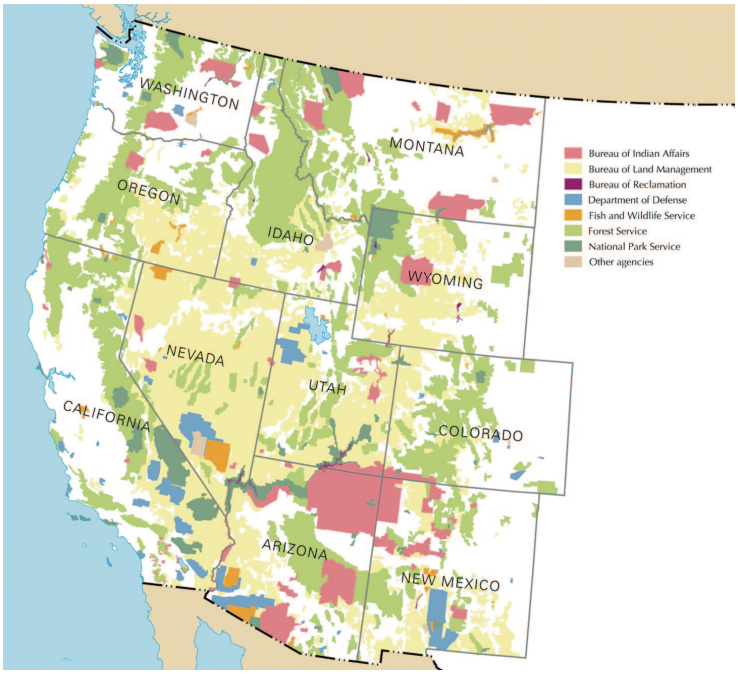

Figure 1. Federally managed land in the Western United States.

increased by about 300% in the 11 contiguous western states in this period (Westerling et al. 2006). Concomitantly, real average annual suppression costs for the US Forest Service alone have increased by a factor of 2.6 over the last 20 years and have exceeded $1 billion in 3 of the years since 2000, while costs for the Department of the Interior agencies also have increased, exceeding $300 million/year in the four years since 2000, more than double the average of the preceding 6 years (Krista Gebert, Rocky Mountain Research Station, pers. comm., 2005).

In the same period, the variance in annual area burned also has increased; the variance in the last 10years is more than 30 times higher than in the 1970s. Increases in variability in annual area burned and in fire suppression costs pose a serious challenge for federal and state land and resource managers because, although budgets have increased recently, funding still reflects what would likely be spent in an "average" year. Given that average years seldom occur, actual costs tend to fluctuate between low and high extremes. Consequently, the US Forest Service's suppression expenses regularly exceed the annual suppression budget.

Federal and state land and resource managers must be prepared for the worst possible scenarios in every fire season. Thus, increased uncertainty about the scale of the western fire season each year imposes high costs on public agencies to sustain appropriate levels of preparedness. Recent progress in our understanding of the links between climate and wildfire and in our ability to forecast some aspects of both climate and wildfire season severity offers some hope that these costs might be reduced through the increased integration of climate information into strategic planning for fire and fuels management (Westerling 2007). In this article we identify actual and potential uses of climate information and forecasts by wildland fire managers, based on the results of a decision calendar survey of fire and fuels managers in the western United States.

Organization of Fire Management

Wildland fire management in the United States is integrated across agencies by the National Interagency Coordinating Center (NICC) located in Boise, Idaho, and by 10 Geographic Area Coordination Centers (GACC). At the same time, a variety of other national, state, and local agencies continue to perform their own wildland fire suppression and preparedness activities. Federal, state, and local entities charged with wildland fire management include the US Forest Service, US Department of the Interior (USDOI) National Parks Service (NPS), USDOI Bureau of Land Management (BLM), USDOI Bureau of Indian Affairs, USDOI Fish and Wildlife Service (FWS), and state land and resource management agencies. Their wildland fire suppression efforts are supported by the US Department of Commerce National Oceanographic and Atmospheric Administration (NOAA) and National Weather Service (NWS, within NOAA), and the National Association of State Foresters.

More than one-half of the land in the 11 contiguous western United States is managed by federal agencies, encompassing most of the West's wildlands (Figure 1; USDOI 2006). Each agency works at different organizational levels, ranging from federal agency offices in Washington DC and the National Interagency Fire Center in Boise, Idaho, to regional agency offices, GACCs, and local administrative units managing the crews and equipment needed to actually perform fire suppression and fuels management. We use the US Forest Service within the US Department of Agriculture and the NPS within the USDOI as examples to describe the organization of fire management across multiple agencies.

At the local level, federal fire managers, fuels managers, and fire chiefs work within national parks and forests; these units are overseen by regional offices of the NPS and the US Forest Service. The local and regional units report, in turn, to national offices of the NPS and the US Forest Service, which are located, respectively, within the Departments of the Interior and Agriculture.

National parks and forests also coordinate their fire suppression and fuels management activities under the auspices of regional interagency fire management organizations and administrative bodies: the GACCs mentioned previously, and Multi-Agency Coordination Groups, which operate during the peak fire season to coordinate all the resources available in the different agencies to maximize efficiency in fighting wildland fires. Outside of the fire season, most interaction between the national parks and forests and their regional and national offices involves budgeting and planning ac-

tivities. Some planning and fuels treatment work is also coordinated with the GACCs and National Interagency Fire Center (NIFC). A simplified flow chart shows the organizational levels and links of interest in this study (Figure 2).

Fire weather and climate information and forecasts feed into the decision processes at different levels from several sources. At the national level the NWS provides a variety of weather and climate products for use by fire managers. NIFC offices in Boise, Idaho, house the national offices for the center's Intelligence and Predictive Services functions. The NWS regional office in Boise provides a specific Fire Weather Service. At the regional level, the GACCs' Intelligence and Predictive Service functions include gathering and disseminating weather and climate information provided by regional NWS offices, as well as from several of the NOAA-funded Regional Integrated Science and Assessment (RISA) projects; the Program for Climate, Ecosystem, and Fire Applications (CEFA); and from their own fire meteorologists. At the local level, climate and weather information is obtained from the GACCs and the NWS, and, at some parks and forests, from staff fire meteorologists.

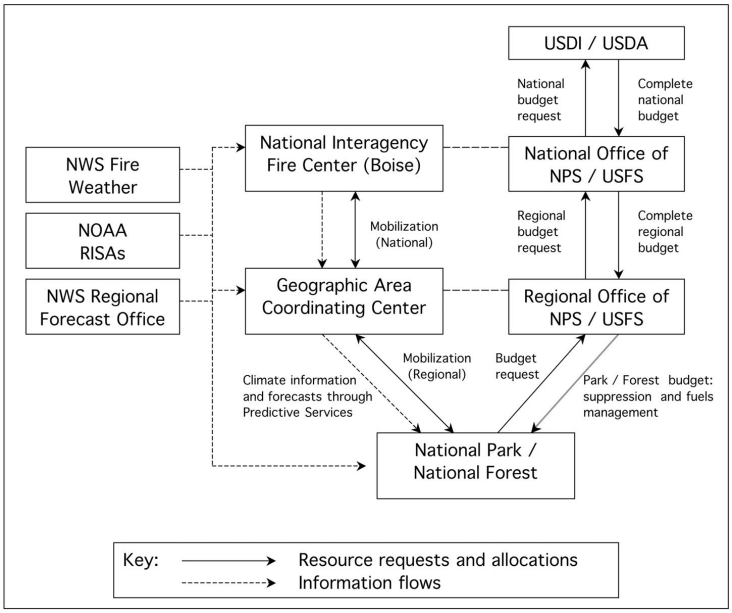

Figure 2. Wildland fire management organizational flow chart.

Climate Science and Climate Forecasts

Over the past several decades, there has been increasing interest in developing a better understanding of the use of scientific and forecasting information by decisionmakers (Hansen et al. 1998, Stern and Easterling 1999, Morehouse 2000, Sarewitz et al. 2000, Jacobs and Pulwarty 2004). Scientific information and forecasts can provide important guidance to decisionmakers who are concerned about reducing risks to vulnerable populations, ecosystems, and the built environment, reducing their operational costs, diminishing the potential for lawsuits or other challenges to their decisions and activities, and managing in a more rational manner the resources for which they are responsible. For example, information about past climatic conditions can prompt decisionmakers to change their assumptions about what constitutes "normal" climatic conditions (Swetnam and Betancourt 1998, Miles et al. 2000, Grissino-Mayer and Swetnam 2000, Westerling and Swetnam 2003); this, in turn, can influence the degree and nature of extreme conditions they include in their infrastructure and emergency planning activities.

Wildfire management is no exception to this recent trend. Traditionally, short-term weather information has been used to great effect operationally in wildland fire suppression during the fire season. With increasingly long and severe fire seasons and with an increased emphasis among federal agencies to restore natural fire regimes to ecosystems through use of fuels treatments such as mechanical thinning, prescribed fires and wildland fire use, seasonal and longer-term climate information products are finding use to support longer-term planning decisions. In this article we identify more opportunities as well as obstacles to further incorporate climate science and forecasts into wildfire management, using decision calendars.

Survey Methods

Decision calendars, as we define them here, are temporally organized structures that reflect the timing of planning and decisionmaking in the course of a regular fire year. Decision calendars have been used previously in integrated climate assessments. We based our calendar format on that used by Wiener (2004). Using this approach allowed us to determine what sorts of plans and decisions were important at which times of the year. This in turn allowed us to associate the timing of decisions, historical climate conditions during those periods, and forecasts for those time periods.

To construct fire management decision calendars showing the use of climate information, we conducted a survey (in 2002–2003) of nine fire management officers and decisionmakers based in the Southwest and California and of several dozen members of wildland fire management groups. We focused on two of the primary federal agencies responsible for wildland fire management, the US Forest Service and the NPS. We structured our selection of interviewees to assure representation of the three most important organizational levels of management: the local level, the regional level, and the national level. Conversations with several key decisionmakers responsible for interagency coordination provided supplemental background information.

The survey was designed to gather a range of information. First, we asked respondents to complete a decision calendar, specifying when during the fire year key prevention and suppression decisions are made and indicating the extent to which climate information and climate forecasts are used

to support these decisionmaking processes. We asked informants to specify what climate information and climate forecasts are used, where these products are obtained, and what additional climate products managers would find useful. We asked respondents about their perceptions of the limitations of these products, in terms of the accuracy of forecasts and in terms of other constraints in the decision processes. We asked if agencies kept records of yearly management goals and of postseason evaluations and if respondents could provide examples of climate information successes and failures. Finally, we asked respondents to rank a set of wildland fire management objectives in terms of importance and to list additional objectives not listed in our survey.

We recognize that the small number of parks and forests we surveyed in the Southwest and the Pacific Southwest happen to have high levels of prescribed fire activity. However, the framework we use could readily be extended to generate a more complete picture of climate information use for fire and fuels management throughout the United States. We also recognize that the number of respondents was too low to conduct a statistical evaluation of responses; however, qualitative analysis produced valuable insights from key informants as well as information that could be generalized across all fire management groups in the US Forest Service and Park Service.

Survey Results

Decision Calendars. The decision calendars (Figure 3) developed from information provided by our respondents show several interesting patterns. The timing of activities varies over the geographical extent of our study areas. In particular, the peak suppression season differs in length and actual time of year from region to region. Southern California has a long season with a special concern in the late fall/early winter season when strong Santa Ana winds are dominant (Keeley 2004, Westerling et al. 2004). The Sierra Nevada in central and northern California has a relatively short season in comparison, while the severity and length of New Mexico and Arizona fire seasons depend heavily on the prefire season precipitation, during-season temperatures (Crimmins and Comrie 2004), and on the timing and wetness of the June–August monsoon season. Of particular concern is the probability of dry lighting igniting fires in the premonsoon period. Monsoon rains typically end the spring/summer fire season (Swetnam and Betancourt 1990), although a second fire season may occur in the fall after the end of the monsoon season. Similarly, optimal windows for prescribed fire and fuels management activities also vary greatly across the study areas.

Figure 3. Aggregated decision calendars.

The decision calendars also differ across organizational levels. At the local level, staffing decisions involve seasonal staffing, training, and determination of hiring and layoff dates. Budgeting involves the internal allocation of funds, annual funding requests, and peak season severity funding requests. Presuppression activities include fuels treatments, prescribed fire, broadcast burns, pile burning, and mechanical thinning projects. Suppression activities include the prepositioning of local resources, movement of resources, mutual aid decisions, severity requests, large fire management and fire use (planning and implementation), fire prevention, restrictions, and area closures. Other local activities reported by survey respondents include outreach, public education, special staffing, training, 5-year planning and analysis, and geographic information system (GIS) analysis.

Regional- and national-level activities include suppression support for large fires or multiple fire events or widespread high fire danger or preparedness levels, strategic prepositioning and movement of resources (again, generally when high danger conditions are present), planning and budgeting work, and the dissemination of information. Research and changes in overall organizational structure are managed at the national level.

Priorities. In accordance with national firefighting policy, risks to lives was consistently ranked as the highest priority by all respondents. Risks to property generally ranked second, although occasionally these risks ranked below smoke management requirements. The priority ranking of other issues, such as the Endangered Species Act (ESA), urbanization, population growth, exotics, and the protection of cultural resources, varied among the respondents. Budget generally placed fairly low on the list of priorities. This owes mainly to the fact that managers view their planning budgets as fixed for a given fire season and that for suppression purposes, severity funding (emergency funding distributed independently of annual budget allocations) ensures that the most important suppression objectives will be met.

Climate Information and Forecasts. The general use of climate information and forecasts to support fire and fuels management activities was described by one respondent as a "funnel approach" with historic data, real-time information, and short-term forecasts (spot forecasts, 1- to 5-day-ahead forecasts) of weather conditions at the narrow end of the funnel, and seasonal and annual outlooks and assessments at the wide end. Longer-term forecast products are used in strategic planning for a wide range of decision processes, including fuels treatment

programs, staffing decisions, resource requests, and budgeting. Throughout the course of the fire season, outlooks and assessments are updated with more accurate shorter-term forecast products. Year-to-date conditions are compiled and compared with historical climate averages. When climate and fuels conditions exceed certain thresholds relative to historic conditions, more active monitoring and management activities are initiated.

According to interviewees, real-time climate information and short-term forecasts used include temperature, humidity, precipitation, fuel moisture, and wind patterns. Forecasts for more than 1 week ahead include drought indices (e.g., Keetch-Byram Drought Index and Palmer Drought Severity Index) soil moisture, live moisture, relative greenness (Normalized Difference Vegetation Index), precipitation, snowpack, fuel moisture, 1,000-hour fuel, live woody fuel (chaparral), Energy Release Component, wind patterns, 30-day outlooks, 90-day outlooks, and 3-year cumulative comparisons. Long-term forecasts used for planning include long-term outlooks for pest management, forest health projects, drought indices, and snowpack.

Sources of climate information identified by respondents included NOAA/NWS regional offices, GACCs websites and meteorologists, BLM's weather site, Desert Research Institute (CEFA), the Remote Automated Weather Stations network for up-to-date readings in the field, and the NICC's Predictive Services websites. The variety of sources reported suggests that fire and fuels managers could potentially benefit from one centralized clearinghouse for information; the clearinghouse could include specialized forecasts and information products for specific geographic areas.

Forecasts a week to a month ahead are used in broad project implementation. They are used in prescribed fire project planning and in burn plan implementation. Such forecasts also are used to support decisions about mutual aid, determining how many resources can be sent to other areas, staffing decisions, prepositioning decisions, and in the request and provision of additional resources. They are used in prevention efforts (e.g., in park or forest closure decisions) and also in severity funding requests.

Responses concerning longer-term seasonal, annual, and interannual forecasts were mixed. Some respondents reported that long-term climate forecasts are used to predict fire season start and end and are considered when planning the next year's projects, e.g., in determining the number of stations to be covered and staffing levels. Many, however, reported that longer-term forecasts still were not accurate enough to be used in decision support. One respondent claimed the use of long-term forecasts was "very rare," another said they "would use, but no product is available," and one respondent voiced concern that "the accuracy [of such products] is just not there yet." Several respondents said they would use long-term climate forecasts if good products were available and, indeed, were generally enthusiastic about the development of such products. Respondents reported that trends are considered in decisionmaking, but also noted that specific long-range forecasts still are not useful to fire and fuels managers. As an example, one respondent mentioned that El Niño Southern Oscillation (ENSO) forecasts that give reasonable information about whether the winter will be wet or dry are not sufficient for management purposes, that what is needed is an indication of how wet the season will be and the timing of the onset of precipitation.

Potential for Improved Use of Climate Information: Planning, Budgeting, Staffing, and Fuels Treatment

Based on survey responses, we have identified a number of decision processes that would benefit from enhanced use of climate information. All the decision activities described below at some point require plans and action with regard to assembling and allocating resources. Hiring, training, and staffing decisions are made leading up to the fire season; the number of fire fighters and support personnel needed are identified for each fire event, vendors are contracted to provide support services, and aircraft and other equipment needs are addressed. These types of activities within an annual decision calendar highlight decision nodes and the entry points where climate and related scientific information may be most readily and effectively introduced. Climate information and forecasts provided in advance of these points are most likely to improve district and forest-level fire management planning, budgeting, and decisionmaking.

National Level. At the national level (i.e., at the NIFC and Washington DC offices of the NPS and US Forest Service), national annual and interannual budget requests and allocations are conducted in the late winter and early spring. Budgeting procedures could be improved by explicitly taking seasonal to interannual climate forecasts into consideration, as could communications with Congress throughout the fiscal year. Forecasts of wildfire season area burned can be made with reliable confidence a year or more in advance in parts of the Southwest, up to a year in advance in some interior basins, and up to a season in advance in many other parts of the western United States (Westerling et al. 2002, 2003, 2006). Thus, forecasts and other information can provide support for annual budget requests for fire management and at the seasonal level for emergency funding requests.

As the fire season approaches, shorter-term climate information provides decisionmakers with information that is useful for refining plans for suppression activities, for identifying opportunities for fire use (i.e., allowing already-ignited fires to burn in areas where such burns would be beneficial to the landscape), and for allocating resources. Fiscal-year suppression-expenditure estimates, which are based on observed and forecasted climate and are updated on a regular basis throughout the fire season, also are used to keep the US Department of Agriculture and Congress apprised of funding needs.

For longer time horizons, instrumental and paleo records can provide analogous scenarios that can be used to explore the possible extent in space, time, and impact of extreme conditions that might affect fire regimes in wildlands. Such information can be incorporated into long-range forest and fuels planning, such as the National Fire Plan, which requires planning out 10 years (US Departments of Agriculture and Interior 2001), and Fire Management Plans, which are revised on a 5-year cycle in conjunction with land-management plans.

Also, in considering long-term objectives, at the national level the Joint Fire Science Program Board sets the national wildland fire research agenda. A greater emphasis on climate information systems and the role of climate forecasts in wildland fire management decisions could lead to improvements in the quality of forecasts available to wildland fire managers.

Regional Level. At the regional level (regional offices of the NPS, US Forest Service, and the GACCs), regional budgeting and resource allocation activities occur be-

fore and during the fire season. Annual hiring, training, and staffing decisions are made leading up to the fire season, as are decisions concerning the prepositioning of initial attack resources. External budget requests at the local level are made annually a year in advance, to regional offices, and could be set more accurately with the aid of annual climate forecasts, potentially reducing the need to rely on severity funds during the peak season. These decision processes could benefit from increased use of seasonal and annual climate forecasts.

The allocation of resources to fire suppression and prescribed fire activities occurs throughout the year, and regional mobilization decisions and mutual aid decisions are made during the peak fire season. Climate information for the past several years and for the upcoming season or year can help managers determine the relative risk of performing prescribed burns, based on current and predicted conditions. For example, managers can compare existing conditions with those of analogous years in the past, based on analyses of the instrumental and proxy records of fire occurrence and climate conditions in the region. Forecasts provide insights into the likelihood of anomalous wet or dry conditions, as well as of "normal" conditions (i.e., those that were statistically prevalent over recent decades).

Institutional Barriers to Using Seasonal Forecasts in Fire Management

The complex set of priorities faced by decisionmakers at each level of wildland fire management suggests that those designing and disseminating climate products need to take into account the different priorities of decisionmakers. In addition to having multiple objectives, decisionmakers also face several constraints. By looking closely at the constraints of decisionmakers, which we identify here, climate scientists can do a better job of developing products that match decisionmakers' needs.

Several important institutional barriers exist to the use of seasonal forecast information by fire managers. First, the 2-year budget cycle for the US Forest Service allows little latitude for shifting funds targeted to forest treatment activities, based on climatic conditions that arise after budgets are submitted and approved. For example, given the high probability of La Niña conditions producing anomalously dry conditions during the winter in the Southwest (Gershunov and Barnett 1998), a reasonably confident La Niña prediction the winter before a fire season should prompt a new analysis of budget allocations to address the emerging fire risk for that season. However, current policies afford little room for such adjustments to allocations of funds to avert or suppress fires in the region.

Second, and related to the first constraint, is the lack of flexibility in authorizing legislation, at the federal level, to make regional or local-level modifications in policies that reflect ground-level realities. For example, fire managers argue in their survey responses that it should not be so cumbersome to obtain permission from the USFWS to treat areas protected by the ESA.

A third barrier to effective use of available climate information and forecasts lies in the lack of flexibility in the fire planning process itself. Organizational inertia is partly to blame. As Lach et al. (2003) have shown for water managers, changes only tend to be made when extraordinary conditions result in the inability of existing practices and policies to address the problems. For example, seasonal staff can only be hired for 6 months in a given year, while in some regions, under certain climatic conditions, the fire season extends beyond 6 months, e.g., Southern California in dry years.

The fourth area of constraints involves the mismatch between decision calendar needs and forecast time horizons. A recurring theme that arose in the surveys and in the interviews was the lack of forecast products specifically targeted to fire and fuels managers. Several respondents stressed the importance of their local topography and its interaction with climate, fire history, and value at risk, and argued strongly for integrating climate forecasts with GIS products that map their region and highlight the condition and location of fuels of particular interest. Local fuels managers reported that 2-week-ahead forecasts would be most useful for planning prescribed burn activities.

Finally, even good forecasts will not be correct every time. Although there are clear benefits to taking early action (e.g., mobilizing resources in advance of a fire event) on the basis of a correct forecast, such benefits often are difficult to measure. The costs of mobilizing resources on the basis of an incorrect forecast, however, are very clear and easy to quantify. As a result, fire and fuels managers are understandably wary of taking proactive measures based on forecast products, unless the accuracy of the forecasts has been proven. Keeping detailed records of forecasts, actions, and outcomes would expedite the development and adoption of new forecast products.

Conclusions

Climate information is currently widely used by fire managers, but there is potential for greater and more effective use of available information, especially if institutional barriers could be loosened. For example, climate forecasts could be used to set more realistic fuels management goals at the unit level and to strategically set priorities for fuels management and prescribed fire treatments. Additional research concerning wildland fire budgeting procedures at the local, regional, and national levels, to identify changes that would facilitate more effective use of climate information would be useful. If congressionally allocated funds could be spent for prescribed burns and other treatments over multiyear time horizons or if tradeoffs in funding could be made over larger regions, it would be easier for managers to adjust their fire and fuels management plans to reflect forecasts and impacts of ENSO conditions, including multiyear combinations of wet and dry conditions. Determining a feasible way of implementing such changes could generate significant efficiency gains.

The National Fire Plan notes that "Critical to fire science program success are mechanisms to ensure that the information is transferred to land and fire managers in a usable form" (US Departments of Agriculture and the Interior 2001). The National Wildfire Coordinating Group's (NWCG) Fire Environment Working Team has been charged in part with assessing current and projected requirements for fire weather products. In this task, continued collaboration between the NWCG and the GACCs with Regionally Integrated Science Assessment project members and other scientists having expertise in climate and wildland fire will be important over the coming decades. Additional training in the use of climate information could be provided through the National Advanced Fire and Resource Institute at the national level (where climate is an explicit topic in the advanced fire danger course), and Predictive Services at the GACCs is ideally suited for disseminating information and skills into operations and planning.

For the climatology community, we expect continuing collaborations with the fire

community to result in the development of better and more useful products to stakeholders. Recent efforts to establish annual fire-climate-fuels assessment processes for the US West and the US Southeast, e.g., included the development of specific consensus climate forecasts for the time periods of most concern to fire and fuels managers, particularly those associated with preseason planning for resource allocation (Garfin and Morehouse 2001, Garfin 2002, Garfin et al. 2003). The National Seasonal Assessment Workshops initiated by the Climate Assessment for the Southwest RISA, CEFA, and Predictive Services offer an annual venue for sustaining communications between producers and users of fire-climate information. (Crawford et al. 2006, Heffernan et al. 2007)

Realizing the full potential of climate information and forecasts will require the collaborative effort of several agencies and the climate science community. The potential gains from such an effort would be significant, however, and can be facilitated by a detailed understanding of the decision-making processes involved in wildland fire agencies, the timing of such decision processes, and the kinds of information requested by fire managers across the United States.

Literature Cited

CRAWFORD, B., G. GARFIN, R. OCHOA, R. HEFFERNAN, T. WORDELL, AND T. BROWN. 2006. *National seasonal assessment workshops, final report June 2006.* Available online at www.ispe.arizona.edu/climas/conferences/NSAW/publications/NSAWproceedings_06.pdf; last accessed July 16, 2007.

CRIMMINS, M.A., AND A.C. COMRIE. 2004. Wildfire-climate interactions across Southeast Arizona. *Int. J. Wildland Fire* 13:455–466.

GARFIN, G.M. 2002. *Fire in the West workshop*. Available online at http://www.ispe.arizona.edu/climas/ conferences/fire.html; last accessed July 16, 2007.

GARFIN, G.M., AND B.J. MOREHOUSE. 2001. *Proc. of conf. on 2001 fire and climate workshops*, Feb. 14–16, 2001, Mar. 28, 2001. CLIMAS, University of Arizona, Tucson, AZ. 75 p.

GARFIN, G.M., T. WORDELL, T. BROWN, R. OCHOA, AND B.J. MOREHOUSE. 2003. *National seasonal assessment workshop. Final report*, Mesa, AZ, Feb. 25–28, 2003. Institute for the Study of Planet Earth, University of Arizona, Tucson, AZ. 24 p.

GERSHUNOV, A., AND T.P. BARNETT. 1998. Interdecadal modulation of ENSO teleconnections. *Bull. Am. Meteorol. Soc.* 79(12):2715–2725.

GRISSINO-MAYER, H.D., AND T.W. SWETNAM. 2000. Century-scale climate forcing of fire regimes in the American Southwest. *Holocene* 10(2):207–214.

HANSEN, J.W., A.W. HODGES, AND J.W. JONES. 1998. ENSO influences on Agriculture in the southeastern US. *J. Climate* 11(3):404–411.

HEFFERNAN, R., T. WORDELL, R. OCHOA, T. BROWN, AND G. GARFIN. 2007 *National seasonal assessment workshop for the Western States and Alaska*. Available online at www.nifc.gov/nicc/predictive/outlooks/NSAW_fullreport_2007_final.pdf; last accessed July 16, 2007.

JACOBS, K., AND R. PULWARTY. 2004. Climate, science, and decision making. P. 177–204 in *Water, Science, Policy, and Management,* Lawford, R., et al. (eds.). Am. Geophys. Union Monogr. Am. Geophys. Union Press, Washington DC.

KEELEY, J.E. 2004. Impact of antecedent climate on fire regimes in coastal California. *Int. J. Wildland Fire* 13(2):173–182.

LACH, D., H. INGRAM, AND S. RAYNER. 2003. Coping with climate variability: Municipal Water agencies in Southern California. P. 59–81 in *Climate and water: Transboundary challenges in the Americas*, Diaz, H.F. and B.J. Morehouse, (eds.). Kluwer Academic Publishers, Dordrecht, The Netherlands.

MILES, E.L., A.K. SNOVER, A.F. HAMLET, B.M. CALLAHAN, AND D.L. FLUHARTY. 2000. Pacific Northwest regional assessment: The impacts of climate variability and climate change on the water resources of the Columbia River Basin. *J. Am. Water Resourc. Assoc.* 36(2):399–420.

MOREHOUSE, B.J. (ED.). 2000. *Proc. of conf. on The implications of La Niña and El Niño for fire management Feb. 23–24, 2000.* CLIMAS, University of Arizona, Tucson, AZ. 46 p.

SAREWITZ, D., R. PIELKE, JR., AND R. BYERLY, JR. (EDS.). 2000. *Prediction: Science, decision making, and the future of nature*. Island Press, Covelo, CA. 405 p.

STERN, P., AND W.E. EASTERLING. 1999. *Making climate forecasts matter.* National Research Council/National Academy of Sciences, Washington, National Academy Press, Washington, DC. 175 p.

SWETNAM, T.W., AND J.L. BETANCOURT. 1990. Fire-Southern Oscillation relations in the Southwestern United States. *Science* 249:1017–1020.

SWETNAM, T.W., AND J.L. BETANCOURT. 1998. Mesoscale disturbance and ecological response to decadal climatic variability in the American Southwest. *J. Climate* 11:3128–3147.

US DEPARTMENTS OF AGRICULTURE AND THE INTERIOR. 2001. *A collaborative approach for reducing wildland fire risks to communities and the environment: 10-Year comprehensive strategy.* US Departments of Interior and Agriculture, in collaboration with the Western Governors Association. Available online at www.fireplan.gov/reports/7–19-en.pdf; last accessed July 16, 2007.

US DEPARTMENT OF THE INTERIOR (USDOI). 2006. *National atlas of the United States*. Available online at nationalatlas.gov/mld/fedlanp.html; last accessed July 16, 2007.

WESTERLING, A.L. 2008. Climatology for wildfire management. Chapter in Economics of Forest Disturbance: Wildfires, Storms, and Pests. Holmes T.P., J.P. Prestemon and K.L. Abt, (eds.). Springer-Verlag, Dordrecht, The Netherlands. (in press).

WESTERLING, A.L., A. GERSHUNOV, D.R. CAYAN, AND T.P. BARNETT. 2002. Long Lead statistical forecasts of Western U.S. wildfire area burned. *Int. J. Wildland Fire* 11(3,4):257–266.

WESTERLING, A.L., T.J. BROWN, A. GERSHUNOV, D.R. CAYAN, AND M.D. DETTINGER. 2003: Climate and wildfire in the Western United States. *Bull. Am. Meteorol. Soc.* 84(5):595–604.

WESTERLING, A.L., AND T.W. SWETNAM. 2003. Interannual to decadal drought and wildfire in the Western United States. *EOS Trans. Am. Geophys. Union* 84(49):545, 554–555.

WESTERLING, A.L., D.R. CAYAN, T.J. BROWN, B.L. HALL, AND L.G. RIDDLE. 2004. Climate, Santa Ana Winds, and Autumn Wildfires in Southern California. *EOS Trans. Am. Geophys. Union* 85 (31):289–296.

WESTERLING, A.L., H.G. HIDALGO, D.R. CAYAN, AND T.W. SWETNAM. 2006. Warming and earlier spring increases Western U.S. forest wildfire activity. *Science* 313:940–943.

WIENER, J.D. 2004. *Small agriculture needs and desires for weather and climate information in a case study in Colorado.* AMS 2004 Users Conference Pre-print, American Meteorological Society, Seattle, WA. 47 p.

Acknowledgements

Chapter 1, in full, is a reprint of the material as it appears in Exploring Use of Climate Information in Wildland Fire Management: A Decision Calendar Study, 2008. Corringham, Thomas W.; Westerling, Anthony L.; Morehouse, Barbara J., Journal of Forestry, 106(2): 71-77. Tom Corringham was the primary investigator and author of this paper.

The Effect of El Niño on Flood Damages in the Western United States

Thomas W. Corringham and Daniel R. Cayan

Abstract

This paper analyzes a novel source of data to quantify the economic impacts of flooding across the western United States from 1978 to 2007. We present a spatial and temporal analysis of National Flood Insurance Program (NFIP) daily claims and loss data over this period. NFIP losses, aggregated over the western US are considerably smaller (only 3%) than broader measures of direct losses measured by a National Weather Service (NWS) data set, but are highly correlated to the annual losses in the NWS dataset. The NFIP data reveals that a small number winter-season extreme hydrologic events, covering wide spatial areas, are responsible for a large proportion of total losses. Furthermore, connections between extreme hydrologic events and the El Niño Southern Oscillation (ENSO) that have been documented in past research are borne out in this record of insurance claims and losses. In coastal southern California and across the southwest, El Niño conditions have had a strong effect in producing more frequent and higher magnitudes of insured losses while La Niña conditions significantly reduce both the frequency and magnitude losses. In the Pacific Northwest, the opposite pattern appears, though the effect is somewhat weaker, and less spatially coherent. The persistent evolution of ENSO offers the possibility for property owners, policy makers, and emergency planners and responders that unusually high or low flood damages could be predicted in advance of the primary winter storm period along the

West Coast. Within the 30-year NFIP history, it is found that the Multivariate ENSO Index would have provided a six month look-ahead for heightened damages in southern California.

1 Introduction

Flooding is the most common and damaging natural disaster in the United States (NOAA 2018). Billions of dollars have been spent to reduce the impact of the flood hazard in communities across the country (U.S. Army Corps of Engineers, 2009). In spite of these efforts, the average annual economic costs of flooding in the United States have continued to rise. From the 1940s to the 1990s, direct flood losses increased fivefold from $1 billion to $5 billion annually, adjusting for inflation (Pielke and Downton 2000). Several factors are responsible for the increasing trend in flood damages, including population growth, income growth, and increased migration towards coastal areas (Changnon *et al.* 2000, Glantz 2001). There is evidence that global climate change is partly responsible, through increased frequency of hurricanes and tropical storms, and an intensification of the hydrologic cycle (Karl and Knight 1998, Groisman *et al.* 2005). It is unclear whether federal policies have aggravated the flood problem, or whether the increases in damages have occurred in spite of the success of these programs (Kunreuther 1998, Sylves and Waugh 1996). Coming to substantive conclusions is difficult, due to the lack of consistent data on flood damages and exposure (Changnon 2003), though the increase in losses in the U.S. appears to be driven largely by increased exposure, *i.e.* increased population and wealth in areas at risk of flooding (Changnon et al. 2000, Downton *et al.* 2005, Pielke *et al.* 2002).

An established body of climate research demonstrates the effects of large-scale atmospheric-oceanic oscillations on hydrologic conditions in the western United States (e.g. Dettinger *et al.* 2000, Gershunov and Barnett 1998). The El Niño Southern Oscillation is a

recurring inter-annual global pattern of ocean-climate variability, driven by sea surface temperature and air pressure differentials in the tropical Pacific (Philander 1990). The boreal winter signature phases of the oscillation, El Niño and La Niña, are associated with floods, droughts, and weather disturbances globally.

As they affect North America, El Niño episodes are associated with a deepened, southward-extended Pacific low-pressure system, a persistent extended Pacific jet stream, and an amplified storm track that produces unusual wetness across the southern tier of the U.S. In contrast, La Niña episodes typically feature anomalous high pressure over the North Pacific, a variable Pacific jet stream, cool and wet weather in the Pacific Northwest and south of the Great Lakes, and unusually dry and warm weather across the southern tier of the U.S. Precipitation in the southwest United States is significantly enhanced in the El Niño phase, and diminished in the La Niña phase of the oscillation (Redmond and Koch 1991). Beyond seasonal precipitation and mean streamflow conditions, it has been established that large-scale climate variations, including ENSO, influence extreme precipitation events (Ropelewski and Halpert 1986; Schonher and Nicholson 1989; Livezey *et al.* 1997; Dettinger *et al.* 1998; Gershunov 1998), and extreme hydrologic events (Cayan and Peterson 1989; Cayan and Webb 1992; Kahya and Dracup 1994; Mitchell and Blier 1997; Cayan *et al*. 1999; Higgins *et al*. 2000).

Advances in climate science have led to an improved understanding of the role of inter-annual climate variability in virtually all sectors of the economy. For example, ENSO, which is the dominant mode of inter-seasonal to inter-annual climate variability, is known to influence agriculture, fisheries, human health, and coastal and terrestrial infrastructure (*e.g.* Glantz 2001). In the western United States, El Niño has a well-documented effect in directing and intensifying North Pacific winter storms (*e.g.* Cayan *et al.* 1999; Dettinger et al. 2000). The strong El Niño

events of 1982/83 and 1997/98 have been linked to significantly damaging flooding in southern California, caused by enhanced precipitation, and by increased wave action caused by stronger wind shear in the tropics. Damages have been estimated at over $1b for each of these two events (Changnon 2003).

However, understanding the connection between extreme hydrologic events and the social and economic impacts of related floods has not received as much attention. The lack of economic data on flood damages has limited research on the economic impacts of climate and hydrologic variability (Changnon 2003). Direct measures of trends in flood-plain occupancy levels or in local flood mitigation investments have not been collected or are not publicly available, and previous analyses linking hydrologic factors to economic damages have been limited to annually aggregated loss series, over large spatial areas, relying on the general assumption that trends in population growth and the increase in real wealth have been spatially homogeneous (*e.g.* Sylves 1998; Pielke and Downton 2000). Pielke and Downton (2000) investigated annual NWS reported flood damages at the state and regional level, finding significant links between reported flood damages and a variety of hydrologic measures, including, most strongly, the number of two-day top-percentile statewide streamflow events per year. They concluded that more spatially detailed studies would be useful to quantify the spatially varying effects of climate phenomena such as ENSO. There is also growing concern that natural variability and human-caused climate change may cause changes in the timing and intensity of the regional hydrologic cycle resulting in anomalously extreme hydrologic events. Hence, to inform policy-making, a better quantitative understanding is needed of the connections between such hydrologic extremes and the expected economic costs.

In this paper, we investigate ENSO effects on flood damage over the western conterminous U.S. The key dataset, described herein, is a novel source of flood damage: 30 years (September 1977 to March 2007) of daily claims and insured losses over the western United States from the National Flood Insurance Program (NFIP). The NFIP data, along with associated climate and hydrologic records, reveals a strong regional and temporal structure in the economic impacts of flooding associated with ENSO-related inter-annual climate variability.

2 Methodology

Pielke and Downton (2000) distinguish between hydrologic floods, in which observed stream flow or river stage exceeds some threshold value or percentile, and economically damaging floods that cause injury, loss of life, or damage to real property. Clearly, all floods are hydrologic, but not all floods cause extensive damage to property or loss of life. For a given hydrologic flood, damages or impacts are jointly determined by the magnitude of the hydrologic event and by the level of exposure or vulnerability of real assets located in the affected area.

In the present study, the determination of flooding (and flood damage) is made using an untapped source, through reports from affected residents, specifically subscribers to the National Flood Insurance Program. Although the analyses are tied to claims and payouts of flood damage, there is an underlying conceptual framework that follows a phenomenological chain. This framework links economic impacts (NFIP claims and insured losses) to location-specific, generally slowly time-varying exposure or vulnerability (population density, real wealth, NFIP participation rates and coverage levels), to extreme stream flow and surface runoff, to seasonal and spatial patterns of extreme precipitation that are modulated by location-specific topography and physiography, and to temporally and spatially varying climate variability. In the following

sections we describe these linkages, with attention to the driving climatic patterns, and with ultimate focus on economic impacts.

3 Data

3.1 Loss Data

We obtained NFIP data on flood insurance claims and insured losses, *i.e.* indemnity payments, for the 11 western states of the coterminous United States. The data cover 29.5 years, from October 1977 through March 2007, and contain records of 64,639 claims, and over $824 million in payments. The National Flood Insurance Program (NFIP), established by the U.S. Congress in 1968 (42 U.S.C. 4028), is a federal program enabling property owners to purchase insurance protection against losses from flooding. This insurance provides an alternative to *ex-post* disaster assistance to meet the escalating costs of repairing damage to buildings and their contents caused by floods (*e.g.* Kunreuther 1998) and is part of a broader program designed to reduce exposure to flood risk over the long-term.

The NFIP record provides a unique and previously untapped resource to explore the economic impacts of ENSO across the Western U.S. The fine spatial and temporal resolution of the data allows us to quantify the economic effects of floods, as they relate to a variety of climatic and hydrologic phenomena. As a record of total flood impacts, or even of total direct flood damages, the NFIP data is obviously incomplete. Federal flood insurance is available only for residential properties, and some small business properties, damages to which constitute only a small fraction of total direct losses (Dixon *et al*., 2006). In addition, even in Special Flood Hazard

Areas (areas in which the estimated annual flood risk is at least 1 percent, or one event in 100 years) participation in the Program is far from universal.

Low participation rates in the early years of the program led to a series of reforms designed to encourage residents in high risk areas to purchase insurance (Pasterick 1998). Currently, rates are still estimated at less than 50 percent in the most flood-prone areas, and under 1 percent elsewhere (Dixon *et al.* 2006). Damages caused by floods not covered by the NFIP include damage to infrastructure, such as dams, levees, bridges, roads, highways, and rail lines, damage to public and industrial property, and damage to agricultural property, crops, and livestock. Importantly, NRIP losses do not include secondary or indirect costs of floods, such as reduced productivity, unemployment, or flood-related health costs.

Despite the above shortcomings, a principal advantage of the NFIP data over other available data sources (*e.g.* Sylves 1998; Pielke and Downton 2000) is that it provides a consistent daily record of claims and damages at relatively high spatial resolution. Each claim in the NFIP database is located to the nearest FEMA Community, typically an incorporated area, *i.e.* a census-defined place (city, town, village, county, county remainder, or Native American tribal area). The street address of each claimant is not available, but the NFIP does provide the location of a large number of claims to the nearest census block group (roughly 40,000 claims, or 2/3 of the claims in our data set have block group codes that match the Community coding).

For each claim, the NFIP Claims Data provides the date of loss (the date on which the most significant damage occurred), the location of the property (FEMA Community, and census block group, if available), the occupancy type (single family residential, 2-4 family residential, 5+ family residential, or non-residential), the flood zone in which the property is located, the total payment

for structural damages and contents. In a supplementary data set, the annual number of policies in force, coverage levels, and premium payments is available at the Community level.

As of policy-year 2006, there were approximately 444,000 policyholders in the 2037 participating NFIP Communities in the western 11 States. In 1978 there were less than 144,000 policyholders, while at a peak in 1998 there were over 522,000 policyholders. The total coverage in force, in 2006, was just over $80 billion (in year-2000-USD). Total premiums paid in 2006 were approximately $220 million, or 0.275 percent of total coverage in force. This may seem like a low number. However, expected flood losses are generally far lower than total coverage levels; in most areas severe floods are relatively infrequent, and when such floods do occur most losses are not catastrophic. From 1978 to 2006, losses per water-year over the 11 western states ranged from a low of $643,300 in 1988/1989 to a high of $126 million in 1994/1995. Median losses per water-year were roughly $11.8 million, while average annual losses were $27.5 million. The average policyholder paid $192 for $74,000 in coverage in 1978, and $496 for $180,000 in coverage in 2006 (or $2.60 to $2.75 per $1,000 of coverage respectively).

In several of our analyses we aggregate NFIP data to monthly one half degree gridded data. Claims, claims paid, and insured losses are aggregated monthly to the nearest one half degree. The spatial aggregation for claims is relatively precise. Roughly two thirds of our data are located to the nearest census block group, the other third to the nearest county. We aggregate spatially using block group and county centroids rounded to the nearest half degree. Policies, premium payments, and total coverage in force data are only available annually at the NFIP community level, so are aggregated annually to the nearest one half degree, again rounding community centroid to the nearest half degree. Claims and policy data are then merged together for our analyses.

3.2 Climate Data

As a measure of ENSO climate variability, we use the Wolter and Timlin (1998) Multi-ENSO Index (MEI), which is a measure constructed using sea surface temperatures, atmospheric pressure and wind patterns over the Pacific Ocean. We found MEI to be better correlated with insured losses than either the Southern Oscillation Index or Niño3.4 (results not shown). Of the thirty winters (or extended cool seasons, which we define as the months of October through March) in our sample, average MEI is 0.356. We conduct split-sample analyses of flood insurance claims and insured losses by region against MEI by breaking the cool-season monthly MEI into lower, upper, and combined middle two quartiles, with break points of -0.32 and 0.92. It should be noted that our sample-period of 1978 to 2007 is somewhat biased towards El Niño winters over La Niña winters, hence the samples used in our split-sample analyses bear a strong but not precise correspondence to traditional measures of El Niño, Neutral, and La Niña winters.

4 Results

4.1 Insured versus Total Flood Damages

Given low participation rates in the NFIP in the western U.S., an obvious question is how insured losses compare to total flood damages. To answer this question, we compare the NFIP insured losses, aggregated by state and by water year, to annual reports of statewide damages collected from National Weather Service (NWS) publications (Sylves 1998; Pielke and Downton 2000). A comparison of the magnitudes of these two series from 1983 to 2003 (the years for which both NFIP and NWS data were available), as depicted in Figure 2.1, reveals that NFIP insured losses totaled over the entire western U.S. are well correlated with the NWS yearly damages, with

the Pearson correlation coefficient registering 0.80 between the two series. As an average over 1983-2003, the magnitude of the NFIP damages summed over the 11 western states is 3.3% percent of total NWS -reported losses. Following these results, the NFIP insured losses can be inflated by a factor of 30 to obtain a rough estimate of the total direct impacts. For example, the most significant flood events in our sample (e.g. 12/30/05 and 1/7/95) caused over $7m in damages: this is equivalent to total impacts $2.25b. This estimate seems high but is within the expected order of magnitude of such events, *i.e.* over $1b (Changnon 2003, Perry 2005). The high year to year variability of the area total losses over the 11 states is symptomatic of the extremely episodic nature of the flood losses exhibited at the daily and local-regional level, described in more detail below.

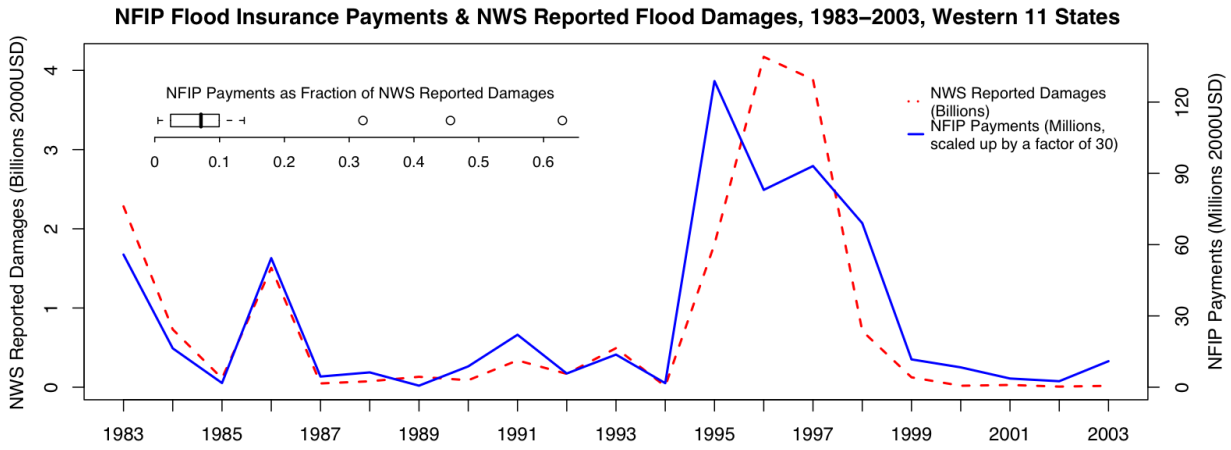

Figure 2.1: NFIP insured losses, NWS reported losses 1983-2003 western 11 states. Annual aggregates of inflation-adjusted NWS damage estimates (dashed red line) and NFIP insured losses (solid blue line) reveal strong coherence (correlation = 0.8).

4.2 Spatial Distribution of Insured Losses

Insured flood damages by county are presented in Table 2.1, which lists the counties with the greatest total insured losses over our sample period, in dollar terms, and relative to number of policies and total coverage. The spatial pattern of losses across the entire Western United States

can be seen graphically in the accompanying Figure 2.2. A strong link between population and losses is apparent, but population is not the sole source of exposure to flood risk. In terms of total damages, many counties in California rank highly, with annual losses exceeding $0.5m. In terms of damages per coverage, the pattern is less spatially coherent. In particular, losses in southern California, which are high in absolute terms, are relatively low in terms of total coverage, or the number of policies. This is likely due to the high population density of southern California and high NFIP penetration levels.

There are some areas, however, that show high damages both in dollar values and in damages per coverage. These include counties surrounding Puget Sound in Washington, and several northern California counties surrounding the San Francisco area. The greatest losses, both in dollars and in dollars per total premium payments, occur in Sonoma County, by no means the most populous area in the Western U.S., but one whose rivers are prone to significant flooding (Ralph 2003).

Table 2.1: Most affected counties: real insured losses; losses per coverage

County	State	Annual Losses (dollars, millions)	Loss per Policy (dollars)	Loss per $100,000 Coverage (dollars)
Sonoma	CA	3.622	1,092	1,130
Los Angeles	CA	2.052	139	101
Marin	CA	1.577	275	213
Sacramento	CA	1.160	56	39
Napa	CA	0.953	560	400
Lewis	WA	0.913	778	990
Washoe	NV	0.905	405	228
Monterey	CA	0.896	443	386
King	WA	0.875	325	269
Clackamas	OR	0.709	302	187
Snohomish	WA	0.603	455	528
Placer	CA	0.546	780	633
Santa Clara	CA	0.541	36	33
Orange	CA	0.531	12	11
Maricopa	AZ	0.495	28	32
San Diego	CA	0.454	94	92
Lake	CA	0.431	366	409
Santa Cruz	CA	0.411	187	269
Ventura	CA	0.407	101	102
Skagit	WA	0.403	132	162
Pierce	WA	0.399	401	396
Riverside	CA	0.390	62	56
Tillamook	OR	0.361	310	272
Cowlitz	WA	0.358	160	128

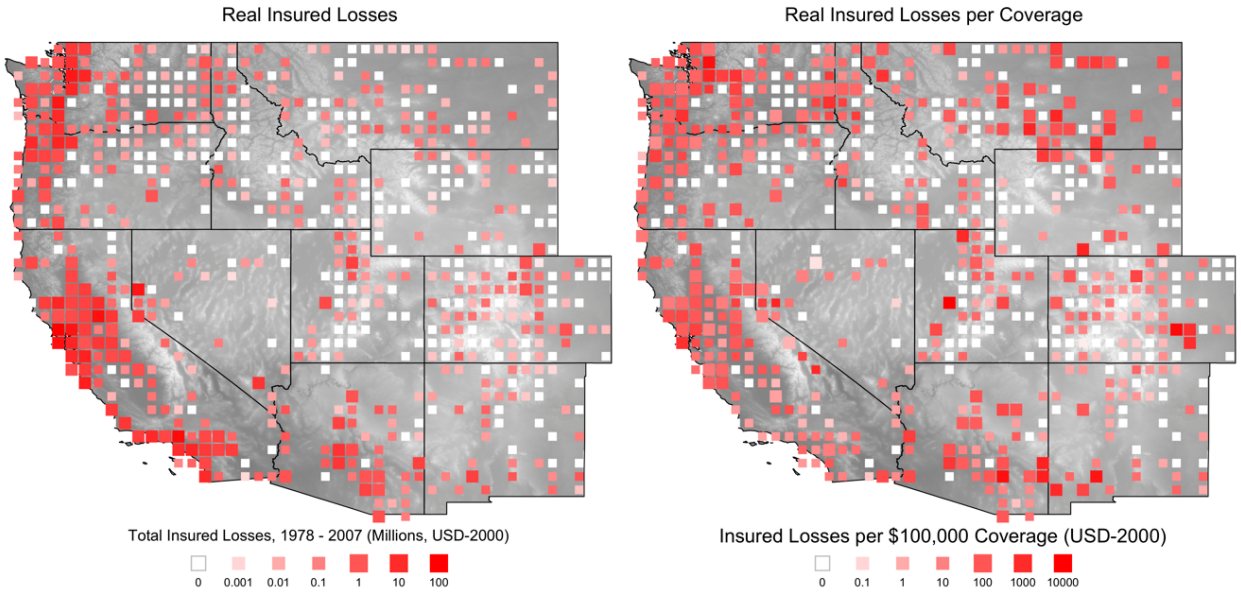

Figure 2.2: Spatial distribution of insured losses; losses per coverage. Total insured losses aggregated spatially over a one-half degree grid are concentrated in developed areas in California, Oregon and Washington. High losses are also observed in Arizona, and in isolated areas throughout the western US. Total losses per coverage adjust for exposure to risk, are still clustered around developed areas, but show a more even distribution across the western US.

Spatial plots of total insured losses aggregated over a finer one-eighth degree grid (not shown) reveal that insured losses are concentrated along the Pacific coast, with large clusters of damages corresponding to the urban areas of Seattle, Portland, the San Francisco Bay Area, Los Angeles, and San Diego. Damages also cluster around river systems, such as the Willamette river system in Oregon, the Columbia River along the border of Oregon and Washington, the convergence of the San Joaquin and Sacramento rivers at Sacramento and the San Francisco Bay Delta, and at the windward bases of orographic mountain ranges such as the Cascades in the Pacific Northwest, the Coastal Ranges from Washington to California, the Sierra Nevada in California, the Transverse Range in southern California, and the Mogollon Rim in Arizona.

Inland real insured losses are uniformly low (Figure 2.2, panel A), while there are many grid points with high losses per coverage in the interior states (Figure 2.2, panel B). We note that

participation rates and number of policyholders are very low in these regions, so we caution against any strong interpretation of these observations.

4.3 History of Insured Losses

Inspection of the time series of daily losses aggregated over the entire western U.S. reveals several points of interest (Figure 2.3). While there is some weak evidence for an increase in total losses over the sample period, once the losses are adjusted for increases in participation and coverage levels, there is no apparent trend in the time-series of insured losses. Perhaps most striking is the highly episodic nature of floods in the Western U.S.: a very small number of extreme events account for a great proportion of total insured losses (Figure 2.3, and Figure 2.3A). Insured flood damages in the Western U.S. display a marked seasonal pattern: the coastal areas dominate the aggregate data with peak losses occurring between November and March (Figure 2.3, inset B).

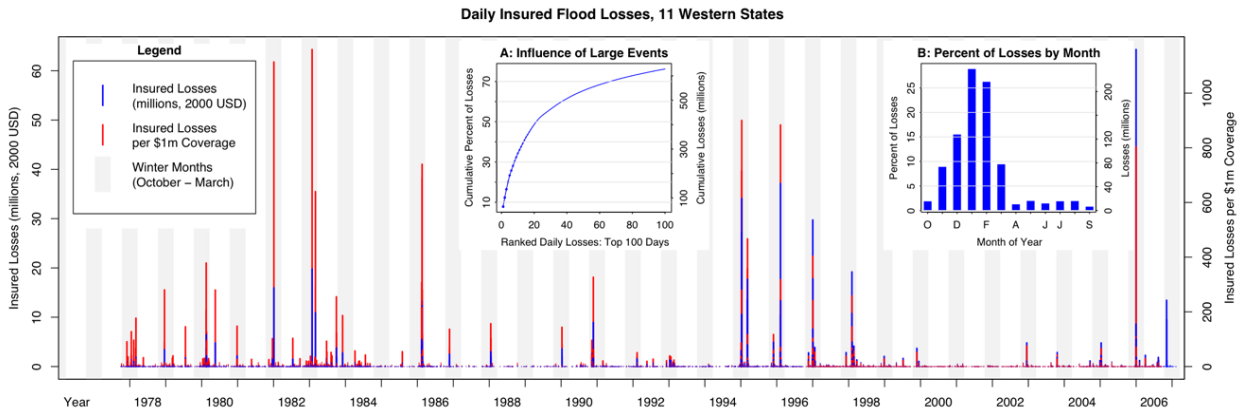

Figure 2.3: Daily time series of insured losses, 11 western states, 1978-2007. Daily time series of insured losses in blue and insured losses per coverage in red reveal the highly episodic nature of damaging floods in the western US. Inset A reinforces this finding showing the fraction of losses accounted for by the top 100 loss days. Inset B shows the seasonal pattern of losses across the western US.

4.3.1 Time Trends

On average, the inflation-adjusted insured losses from the NFIP amount to roughly $27.5m per year ($825m in total impacts), although the record is dominated by a handful of large events. The time series exhibits a slight increasing trend over time: the annual growth rate is 1.84 percent per year from 1978 to 2007 (though, with a standard error of 2.81 percent, the trend is not statistically significant). The red bars in Figure 2.3 represent real insured losses adjusted for the total coverage in force. In this time series of losses per coverage there is actually a slight negative time trend, but it is also not statistically significant.

After adjusting for changes in coverage levels the peak daily losses associated with the floods during 1997-98 El Niño winter, for example, were lower than those associated with the 1982-83 El Niño winter in terms of losses per coverage. This may have more to do with increases in coverage levels over the time period due to increased promotion of the NFIP than to actual differences between the two El Niño events however. Although real insured losses associated with flood events in the Western U.S. have increased over the past thirty years at an annual rate of 1.84 percent, after controlling for increasing population, home values, and coverage levels, we observe that losses have actually declined, or remained stable over the past three decades. Since weather and hydrologic conditions have been essentially stationary in the Western U.S. over the sample period (e.g. Karl and Knight 1998), this may indicate some success of the NFIP program in controlling flood risks in participating communities, through repetitive loss buy-back programs and community flood mitigation efforts.

4.3.2 Influence of Extreme Floods

As seen in Figure 2.3, and displayed in Inset A, a small number of extreme flood events account for a large and disproportionate amount of the total damages over the past thirty years. The top 22 days of losses (constituting 12 separate meteorological events) account for over 50 percent of the total damages in the Western U.S. over the 30-year sample period. Events causing over $10 million in insured losses occur, on average, once every two to three years, though in several cases two such events have occurred over the course of a single water-year or even a single month. Assuming that insured losses account for 3 percent of total damages, this translates into (direct) damages of approximately $300m per event. Though the western U.S. flood loss history is not as pronounced as, for instance, the record of hurricane damages in the Gulf Coast, it does show a similar highly episodic general form.

The five greatest single-day losses occurred, in order of decreasing losses, on December 31st 2005, February 8th 1996, January 10th 1995, January 1st 1997, and January 9th 1995. Table 2.2 presents a list of the 15 most damaging events over the past thirty years, arranged by date, listing the dates of extreme damages, the location, the number of claims, the total real damages, and losses per policy and per coverage. Here we define a single event as a set of consecutive days of losses in a given area. All of the significantly damaging events in our record are characterized by a marked peak loss date. In those cases in which two distinct peak loss dates are observed, the successive peaks are classified as separate events, e.g. 1986/2/12, 1986/2/17, and 1998/2/1, 1998/2/6).

Table 2.2: Flood events with real insured losses in excess of $10m

Event Start Date	Days	Losses (millions)	Communities by Region S.CA	N.CA	OR	WA	All	ENSO MEI
12/30/05	7	82.22	10	112	35	8	172	-0.52
1/7/95	10	76.01	55	114	7	0	181	1.18
2/3/96	10	66.47	5	22	74	80	210	-0.62
12/31/96	7	64.39	9	119	45	49	249	-0.35
3/8/95	5	36.89	40	89	0	1	138	0.78
2/17/86	5	32.76	6	103	3	2	124	-0.24
2/1/98	5	32.53	69	140	0	4	214	2.7
11/2/06	9	25.01	1	1	12	51	66	1.29
1/25/83	6	20.35	37	86	7	7	139	2.72
2/28/83	8	17.24	92	64	2	2	170	2.97
1/1/82	6	16.07	5	77	1	0	86	-0.29
2/12/86	5	14.49	23	77	2	2	107	-0.24
2/13/80	5	12.53	77	25	2	0	128	0.52
11/23/90	6	12.16	0	0	0	58	61	0.38
2/6/98	5	10.99	85	94	0	1	184	2.7

The typical length of a highly damaging flood event in the western US, as measured from trough to trough in damages is five to ten days. Insured losses per event (in year 2000 USD) are as high as $80m, which translates into total impacts in excess of $1b. Obviously the estimate on total impacts is highly imprecise, but the order of magnitude seems plausible given other estimates in the literature (*e.g.* Perry 2005). Losses per coverage in these highly damaging events range from $30 to $200 per $100,000 worth of coverage.

Regionally, these most damaging events cover a wide geographic area, from southern California to Washington. We capture the regionality of events in Table 2.2 by listing the number of NFIP communities with claims during the event by region. The top events are concentrated in northern California, although three of the top fifteen events are associated with significant losses in Washington and Oregon. The link between El Niño and flood damages is explored further below, but there is some evidence of an ENSO influence on losses in these top events. Several of the

events concentrated in southern California are associated with high MEI values, while the top two events concentrated in the Pacific Northwest are associated with low MEI values. Indeed, the strong El Niño events (MEI > 2.7) were all concentrated in southern California. The signal is not perfect, however. Northern California flooding occurs in months with high and low MEI values. The event of 11/2/2006 concentrated in the Pacific Northwest occurs in a month with elevated MEI.

4.3.3 Seasonality of Insured Losses

Insured flood losses display a strong seasonal pattern, as highlighted in Figure 2.3, Inset B, with over 90 percent of total insured losses occurring during the months of October through March, and over 55 percent in the months of January and February alone. This strong winter flood seasonality is dominated by the large events that occur along the Pacific coast. The timing of regional peak flood seasons across the Western U.S. is more variable, following a relatively clear general pattern associated with elevation and latitude, as depicted in Figure 2.4.

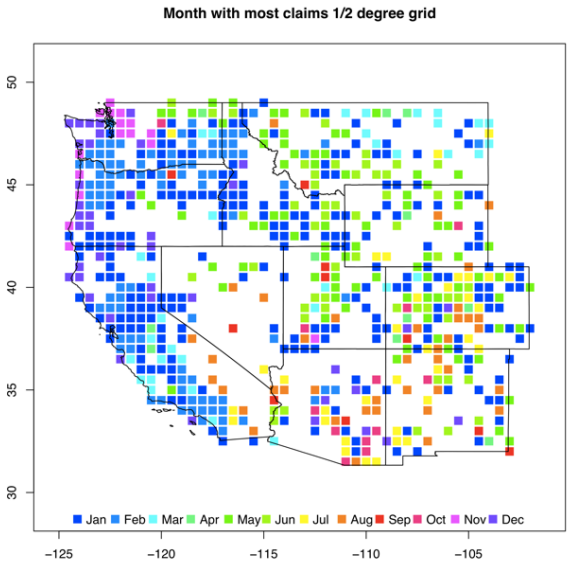

Figure 2.4: Regional seasonality of flood losses: month of year with maximum losses. Total claims were aggregated by month over a one-half degree grid. For each grid cell, the month with the maximum number of claims was noted and is plotted here by color.

The 30 years of NFIP record exhibits a progression of winter peak flood losses along the West Coast, earlier in the winter in the north to later in winter in the south, in accord with the seasonal development and migration of the North Pacific winter storm track (Gershunov *et al*. 2017). November marks the beginning of the peak flood loss season in the Pacific Northwest, with damaging floods occurring to the east of Puget Sound and at various points along the Pacific coast of Washington and Oregon. Damaging winter flooding (December - February) occurs across the entire western U.S. December peak flood losses occur in the Olympic Range of western Washington, and along the Pacific coast of Washington and Oregon, and at some locations in northern California. In January peak flood losses occur in some locations in all 11 western states. Damages caused by January floods are concentrated in central and northern California, especially surrounding the Bay Delta, but reaching eastward as far as western Nevada. February peak flood

losses are concentrated in southern California, some parts of northern California, and along the Columbia River valley from northern Idaho through Washington and Oregon. In March peak flood losses register in a few locations in southern California.

Peak flood losses over the interior West have exhibited a more complicated seasonal pattern than those along the West Coast. Peak Spring flood losses (March - May) occur in locations throughout the interior West. Damaging flooding occurs in the spring in northern Washington east of the Cascades, across Montana, Idaho, Wyoming, northern Nevada, Utah, Colorado, and parts of New Mexico. Summer flood losses (June - August) are relatively rare in the western U.S., and appear confined to the intermountain west, presumably due to smaller scale convective thunderstorm systems. Damaging floods in July and August occur in the desert areas of inland southern California, southern Nevada, and across Arizona, New Mexico, and southern and central Colorado. Fall flood losses (September - November) are concentrated in Arizona, probably a result of the southwest monsoon, remnant tropical storms, and extratropical systems including cutoff lows, with isolated fall flood losses occurring throughout the intermountain west. December, January, and February peak flood damages have occurred, in rather scattered fashion, across the interior West from Arizona and New Mexico northward to Idaho and Montana.

4.4 Climate Linkages

Over a several-decade record, storm events in given regions occur with reasonably well-known frequencies and magnitudes. Superficially their year-to-year occurrences may appear random. But there is a body of research that indicates that large scale climate anomalies affect the frequencies, intensities, and spatial distribution of the storm systems (e.g. Cayan *et al*. 1999; Thompson and Wallace 2001). Here we seek to investigate regional coherence in insured flood

damages and quantify the extent to which ENSO, the most prominent inter-annual climate variability mode, is correlated. We also assess the viability of using ENSO signals in antecedent months to predict flood damages in the Western U.S. The climate linkage analyses are restricted to flood losses during the extended cool season of ONDJFM, since, as shown in Section 4.3, it has contained most (84.4%) of flood losses over the western U.S.

4.4.1 Principal Components Analysis

To characterize the spatial and temporal patterns of flood damages, we conducted a principal components analysis (PCA) of the 30-year NFIP record of flood damages during October-March at a variety of spatial and temporal resolutions. The PCA demonstrates that flood damage tends to occur over rather broad regional footprints, as indicated in Figure 2.5 by the first three empirical orthogonal functions (EOFs) of winter monthly flood losses per coverage, aggregated over a one-half-degree grid, and their associated monthly PC time series. Remarkably, for a process that is considered to occur episodically and often rather locally, the first three EOFs account for over 25 percent of the total October-March monthly variance in flood damages. These patterns, respectively, describe flood damage over the coastal communities of Washington, Oregon, and California, over the Pacific Northwest contrasted with central and southern California, and over coastal Washington and the Southwest contrasted with central and northern California and coastal southern Oregon. The large spatial footprint of flood damages exhibited in the principal component analysis suggests the influence of climate variability on economically damaging floods.

EOF 1, which has same-sign loadings over much of the far western conterminous U.S., represents the overall mean pattern in cool season losses per coverage, as illustrated in Figure 2.5. Factor loadings are highest in northern California. Factor loadings are of the same sign in southern

California and the Pacific Northwest but of lower magnitude, owing to the higher population densities and coverage levels in that region. The PC 1 time series (associated with the EOF 1) is elevated in those years with high losses in the areas of greatest variability of losses. EOF 2 is a pronounced north-south dipole, with enhanced factor loadings in the Pacific Northwest extending eastward through the Columbia River basin into northern Idaho and western Montana. The PC 2 time series exhibit a strong influence of the 1996 La Niña winter, which was associated with the highest Pacific Northwest losses over the 30-year period. PC 2 also factors negatively during El Nino winters such as occurred during 1983, 1998, resulting in it having heightened losses in California and diminished losses in the Pacific Northwest in those years. EOF 3 captures variability orthogonal to the first two factors, with heightened factor loadings in southern California and across the Southwest through Arizona. Here the interpretation of the associated time series is complicated by the fact that this component is orthogonal to the first two, though, like the previous two PCs it demonstrates the same impacts of extreme events.

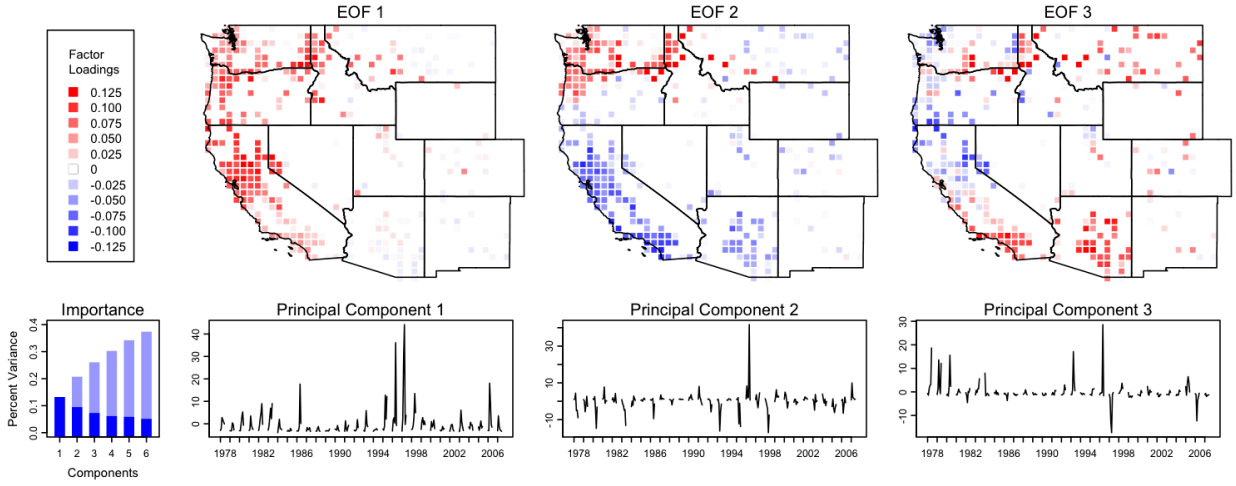

Figure 2.5: PCA: cool season log losses per coverage over one-half degree grid. We plot the first three EOFs and PCs of a principal component analysis of monthly losses per coverage over the extended cool season (ONDJFM), and the total (dark blue) and cumulative (light blue) percent of the variance explained by the first six components.

4.4.2 El Niño and Flood Damage in the Western United States

Because ENSO variability is clearly associated with the defined patterns of anomalous precipitation and flood damages across the western United States, this linkage is explored in greater detail. Composites of winter NFIP flood damages per coverage, conditional on the contemporaneous MEI (Figure 2.6), reveals a strong spatial pattern linking flood damages to the ENSO climate cycle. The El Niño winter months (MEI > 0.92) exhibit a marked increase in damages in coastal southern California, while damages are average or below average in the Pacific Northwest. For the La Niña winter months (MEI < - 0.32) the opposite pattern emerges, with above-average damages in the Pacific Northwest, and below average damages in southern California, and parts of the Southwest. The cut-off values for MEI were chosen to break the sample of 30 years of ONDJFM months into thirds.

The variable plotted in Figure 2.6 is the difference between mean winter monthly losses per $100,000 of coverage by ENSO phase, and the overall winter mean. To assess the significance of the differences we used Welch two-sample *t*-tests by one half degree grid cell. Significance levels of 0.1 are boxed, significance levels of 0.05 are marked with plus signs. We note that the statistical significance of the results is not especially strong, particularly considering issues with multiple testing, but the overall spatial coherence of the areas of significance is striking.

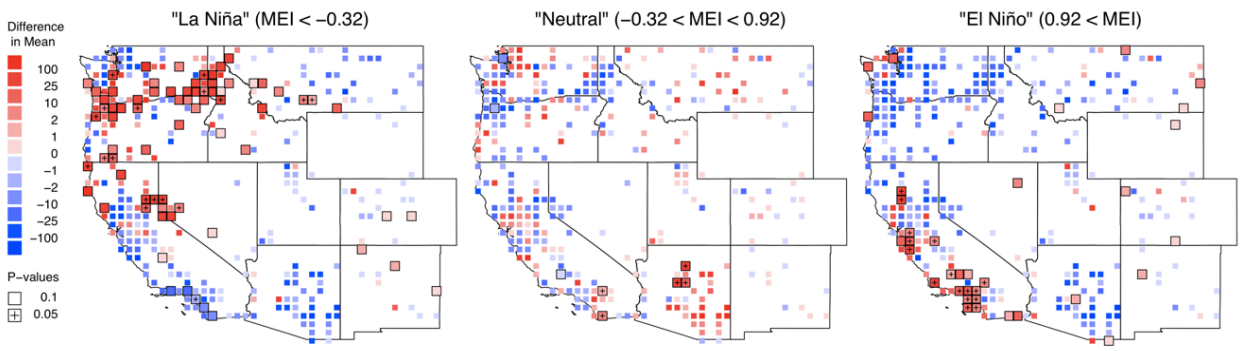

Figure 2.6: ENSO composites, mean ONDJFM monthly losses per $100,000 of coverage. We plot composites of mean ONDJFM monthly losses per coverage over a one-half degree grid. Enhanced losses are colored red, reduced losses in blue, with color intensity on a log scale. Boxed grid cells are significantly different from the overall ONDJFM mean at $p < 0.1$, using a Welch two-sample *t*-test. Boxed cells with crosses are significant at $p < 0.05$.

In the La Niña composite we observe significant increases in losses relative to overall mean in coastal northern Oregon, coastal southern Washington, and inland along the Columbia River basin, extending eastward as far as the Idaho panhandle. There are also scattered areas of significant increases in losses in southern Oregon and northern California. Also notable are increased losses on the leeward side of the Sierra Nevada mountain range in California and surrounding Reno along the Truckee River in Nevada. Losses are significantly lower than normal in southern California during the La Niña phase. Scattered areas of significant differences in New Mexico and Colorado are probably due to low participation rates and low numbers of damaging events.

In the ENSO-neutral composite we see average damages throughout the western U.S. Damages are coherently higher than average in Arizona, with areas of significance in northern Arizona. In northern and southern California, the signal is mixed during the neutral phase. One other area with a notable increase in damages during the neutral phase is the Seattle area east of

Puget Sound. Though not significant, the pattern is spatially coherent, and the area exhibits lower than average losses in both the La Niña and El Niño phases. There is an area of mild increase in losses associated with the neutral phase surrounding the Sacramento area and the San Francisco Bay Delta. We note that the results in the ENSO-neutral panel are somewhat sensitive to the MEI cut-off values.

In the El Niño composite we observe significant increases in losses relative to overall mean in coastal southern California and in the San Francisco Bay Area. North and east of the Bay Area the signal is mixed. In general, northern California appears to incur high damages in strong and moderate El Niño winters and in ENSO-neutral conditions. As a final caveat, we note that the sample size of this analysis is only 30 winters and the record is dominated by two significant El Niño events and one significant La Niña event, significant both in terms of MEI and in terms of damages. The results may change when updated when newer loss data becomes available.

4.4.3 ENSO Prediction of Flood Damages

Given the persistence of different ENSO phases and their influence on flood damages in southern California and parts of the Pacific Northwest, we consider how effectively ENSO indices could be used to predict flood insurance claims or insured losses, and how far ahead such predictions could be made.

In Figure 2.7 we plot ONDJFM cool season losses stratified by ENSO phase by month of year leading up to the cool season. To read the figure, consider the month of September in southern California, labeled as 1 month ahead of ONDJFM. The red curve indicates the average ONDJFM loss per coverage given high MEI Septembers in our sample (MEI > 0.855). Here we see that cool season losses average approximately $100 per $100,000 coverage in those years in which

September MEI is elevated. Mid-MEI Septembers are associated with ONDJFM losses per coverage in the $40 range, while low-MEI Septembers lead to cool season losses of under $10 per $100,000 coverage.

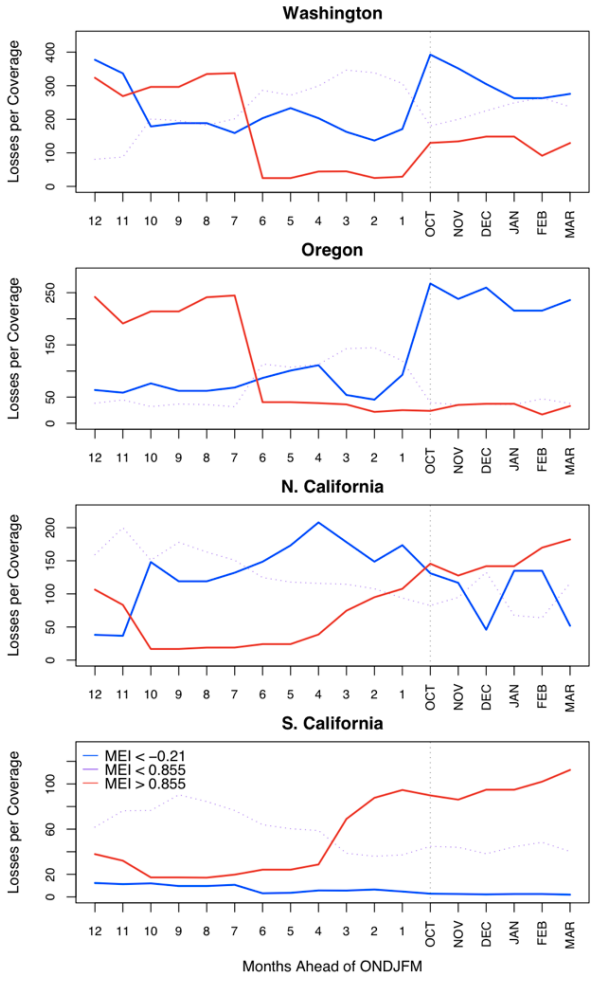

Figure 2.7: Leading MEI values versus losses per coverage by region. ONDJFM mean losses (*y*-axis) are composited on contemporaneous (ONDJFM) and leading (12 to 1 months ahead) measures of ENSO phase (MEI less than -0.21, between -0.21 and 0.855, and greater than 0.855) over four latitude bands.

Interpreting these figures, we see that, within the cool season months, there is a clear contemporaneous correlation between MEI and ONDJFM losses in southern California (high MEI associated with high losses), and Oregon and Washington (low MEI associated with high losses,

stronger in Oregon than in Washington). The contemporaneous signal in northern California is mixed. Losses from $50 to $150 per $100,000 coverage are seen at all levels of contemporaneous MEI.

Looking further, Figure 2.7 provides a perspective on whether antecedent values of unusually high or low MEI status can be used to forecast ONDJFM losses. In Oregon the evidence is weak. One month ahead of ONDJFM, the signal is already mixed; while the contemporaneous correlation between MEI and winter damages is strong, the signal is weaker in September, one month ahead of the cool season damages. Mean cool season losses are slightly elevated when September MEI is low or moderate compared to high MEI, but the effects are modest. A similar pattern is seen in Washington. Interestingly in both Washington and Oregon, positive (El Niño phase) MEI over the antecedent summer months are associated with markedly lower ONDJFM losses than are MEI values that fall into the neutral ENSO phases. This suggests that forecasting winters with high damages in the Pacific Northwest may be difficult, but forecasts of winters with low damages may have more skill.

In northern California the highest winter losses appear to be correlated with low MEI summers. There is some muted evidence for an El Niño signal associated with winter damages, as the highest ONDJFM losses are contemporaneously associated with high MEI values, and the signal gradually appears over the summer months leading up to the cool season. Still, we see that leading low MEI months are associated with the highest winter losses.

In southern California we observe a strong contemporaneous and leading MEI signal associated with losses. The stratification described above in the month of October (three months ahead of the peak loss months in southern California of January through March) is evident as early

as July as the signal grows over the summer months. This suggests that ENSO forecasts up to six months ahead of peak season losses may be possible. Such forecasts would be of considerable value to property owners and policy makers, allowing for mitigation activities to be planned and implemented well ahead of winter seasons with highly damaging extreme storm events.

5 Conclusions

Over the 11 states in the conterminous western United States, NFIP losses amount to about 3 percent of annual losses reported by the NWS. Over the 1978-2007 period, annual losses reported by the NFIP are well correlated with those in the NWS series, indicating that the NFIP insured loss series is an accurate proxy for total losses in the region. The connection between the two series appears strongest in those areas where losses are greatest and where population densities are highest.

An examination of the time series of NFIP losses reveals a highly variable pattern of losses from year to year in all locations that experienced any significant flood activity. This underscores the need for the continued federal provision of flood insurance, as it is unlikely that private insurers would be willing to underwrite such a volatile risk. While many other studies have found that flood losses have been increasing dramatically over time, we find only a modest increase in losses in the western U.S., most of which can be attributed to increased levels of exposure. That is, there is no compelling evidence in this data sample to suggest that the hydrologic cycle has changed significantly in the three decades in our sample in a way that has increased flood damages. The data does suggest that smaller losses have become less frequent, which could be due to improved flood protection investments, the acquisition of repetitive loss properties, or other factors.

While the NFIP flood damage measures have not exhibited marked secular trends, they do contain significant temporal and spatial variability. Flood losses in the western U.S. are highly seasonal, with aggregate losses dominated by the seasonality of losses in the coastal states of California, Oregon, and Washington, where losses are concentrated over the months of November to March. Further inland, the peak flood season shifts from the winter months to the summer months and total losses decrease markedly.

In spite of our short time sample and the fact that ENSO teleconnections are known to waver, we observe a clear fingerprint of ENSO on the history of flood damage in our sample. The patterns associated with ENSO and extreme hydrologic events in the western U.S. carry over very closely to actual economic impacts. The total variation in losses over time in a given region is high. This said, we find that the ENSO phase contributes significantly to this variation in the focal areas of southern California and Arizona, and in the Pacific Northwest, Idaho, and Nevada. In many areas, mean losses in the dominant ENSO phase were several times greater than mean losses in the quiescent phase. Southern California insured losses exhibited the greatest response to ENSO over our sample period, with average losses during El Niño winters of over 20 times as great as losses during La Niña winters.

The fact that average annual losses vary substantially between ENSO phases in certain regions raises the possibility that, as property owners become more sophisticated consumers of climatologic forecasts, they may begin to purchase insurance only in those winters where expected losses are high, which could adversely affect the economic sustainability of the NFIP. In a purely market-based insurance program, one might expect to see insurers varying their premium rates on the basis of long-lead climate forecasts. It is unclear whether such a scheme would be feasible or even desirable for the NFIP. A possible alternative to time-varying premium rates would be a

further strengthening of mandatory purchase requirements, for example requiring continual coverage in high-risk areas, or only offering contracts of durations longer than one year.

Many, if not all, of the extremely damaging flood events identified in this study appear to result from extreme winter extra-tropical storms, often atmospheric rivers (Ralph *et al*. 2006). These events are only weakly aligned with ENSO, which helps to explain why ENSO is an imperfect predictor of flood losses. An improved understanding of these events and their antecedent conditions could provide of advanced warnings and early mitigation efforts. This need is further underscored given that human-caused climate change may result in changes in the timing and increased intensity of extreme hydrologic events (*e.g*. Polade *et al*. 2017).

A significant difficulty in assessing climate risks in terms of extreme flood events is the lack of consistent data on such events. In this study we have demonstrated that NFIP flood insurance data in combination with climatologic data can yield interesting and powerful results. This research demonstrates the utility of such an interdisciplinary approach and can be extended to quantify the social and economic impacts of a wide variety of meteorological and climatological phenomena across the United States. The continued exploration of the links between climatology, hydrometeorology and economic impacts is essential in understanding the impacts of anthropogenic climate change as a driver of extreme events over the coming century.

6 Acknowledgements

Chapter 2, in full, is currently being prepared for submission for publication of the material. Corringham, Thomas W.; Cayan, Daniel R. Tom Corringham was the primary investigator and author of this material. Tom Corringham would like to thank Tony Westerling, Dan Cayan, Richard Carson, and a NSF IGERT fellowship for funding part of his graduate studies.

7 References

Daniel R. Cayan and David H. Peterson. The influence of North Pacific atmospheric circulation on streamflow in the West. In David H. Peterson, editor, Aspects of Climate Variability in the Pacific and the Western Americas, volume 55 of Geophysical Monograph Series, pages 375-397. American Geophysical Union, Washington D.C., 1989.

Daniel R. Cayan, Kelly T. Redmond, and Laurence G. Riddle. ENSO and hydrologic extremes in the western United States. Journal of Climate, 12(9):2881-2893, 1999.

Daniel R. Cayan and Robert H. Webb. El Niño/Southern Oscillation and streamflow in the western United States. In Henry F. Diaz and Vera Markgraf, editors, El Niño: Historical and Paleoclimatic Aspects of the Southern Oscillation, pages 29-68. Cambridge University Press, 1992.

Stanley A. Changnon, Roger A. Pielke, Jr., David Changnon, Richard T. Sylves, and Roger Pulwarty. Human factors explain the increased losses from weather and climate extremes. Bulletin of the American Meteorological Society, 81(3):437-442, 2000.

Stanley D. Changnon. Measures of economic impacts of weather extremes. Bulletin of the American Meteorological Society, 84(9):1231-1235, 2003.

Michael D. Dettinger, Daniel R. Cayan, Henry F. Diaz, and David M. Meko. North-south precipitation patterns in western North America on interannual-to-decadal timescales. Journal of Climate, 11(12):3095-3111, 1998.

Michael D. Dettinger, Daniel R. Cayan, Gregory J. McCabe, and José A. Marengo. Multiscale streamflow variability associated with El Niño/Southern Oscillation. In Henry F. Diaz and Vera Markgraf, editors, El Niño and the Southern Oscillation: Multiscale Variability and Global and Regional Impacts, pages 113-148. Cambridge University Press, 2000.

Lloyd Dixon, Noreen Clancy, Seth A. Seabury, and Adrian Overton. The National Flood Insurance Program's market penetration rate: Estimates and policy implications. Technical report, RAND Corporation, Santa Monica, CA, 2006.

Mary W. Downton, J. Zoe Barnard Miller, and Roger A. Pielke, Jr. Reanalysis of U.S. National Weather Service flood loss database. Natural Hazards Review, 6(1):13-22, 2005.

John A. Dracup and Ercan Kahya. The relationships between U.S. streamflow and La Niña events. Water Resources Research, 30(7):2133-2141, 1994.

Alexander Gershunov. ENSO influence on intraseasonal extreme rainfall and temperature frequencies in the contiguous United States: Implications for long-range predictability. Journal of Climate, 11(12):3192-3203, 1998.

Alexander Gershunov and Tim P. Barnett. ENSO influence on intraseasonal extreme rainfall and temperature frequencies in the contiguous United States: Observations and model results. Journal of Climate, 11(7):1575-1586, 1998.

Gershunov, A., T. Shulgina, F. M. Ralph, D. A. Lavers, and J. J. Rutz (2017),Assessing the climate-scale variability of atmospheric rivers affecting western North America, Geophys. Res. Lett., 44, 7900–7908, doi:10.1002/2017GL074175.

Michael H. Glantz. Currents of Change: Impacts of El Niño and La Niña on Climate and Society. Cambridge University Press, 2nd edition, 2001.

Pavel Ya Groisman, Richard W. Knight, David R. Easterling, Thomas R. Karl, Gabriele C. Hegerl, and Vyacheslav N. Razuvaev. Trends in intense precipitation in the climate record. Journal of Climate, 18(9):1326-1350, 2005.

R. Wayne Higgins, Jae-Kyung E. Schemm, Wei Shi, and Ants Leetmaa. Extreme precipitation events in the western United States related to tropical forcing. Journal of Climate, 13(4):793-820, 2000.

Ercan Kahya and John A. Dracup. U.S. streamflow patterns in relation to the El Niño/Southern Oscillation. Water Resources Research, 29(8):2491-2503, 1993.

Thomas R. Karl and Richard W. Knight. Secular trends of precipitation amount, frequency, and intensity in the United States. Bulletin of the American Meteorological Society, 79(2):231-241, 1998.

Howard O. Kunreuther. Introduction. In Howard O. Kunreuther and Richard J. Roth, Sr., editors, Paying the Price: The Status and Role of Insurance Against Natural Disasters in the United States, pages 1-16. Joseph Henry Press, Washington D.C., 1998.

Robert E. Livezey, Michiko Masutani, Ants Leetmaa, Hualan Rui, Ming Ji, and Arun Kumar. Teleconnective response of the Pacific-North American region atmosphere to large central equatorial Pacific SST anomalies. Journal of Climate, 10(8):1787-1820, 1997.

Todd P. Mitchell and Warren Blier. The variability of wintertime precipitation in the region of California. Journal of Climate, 10(9):2261-2276, 1997.

NOAA National Centers for Environmental Information (NCEI). U.S. Billion-Dollar Weather and Climate Disasters, 2018. https://www.ncdc.noaa.gov/billions/

Edward T. Pasterick. The National Flood Insurance Program. In Howard O. Kunreuther, editor, Paying the Price: The Status and Role of Insurance Against Natural Disasters in the United States, pages 125-154. Joseph Henry Press, Washington D.C., 1998.

S. George Philander. El Niño, La Niña, and the Southern Oscillation. Academic Press, San Diego, California, 1990.

Roger A. Pielke, Jr. and Mary W. Downton. Precipitation and damaging floods: Trends in the United States, 1932-97. Journal of Climate, 13(20):3625-3637, 2000.

Roger A. Pielke, Jr., Mary W. Downton, and J. Zoe Barnard Miller. Flood damage in the United States, 1926-2000 a reanalysis of National Weather Service estimates. Technical report, Environmental and Societal Impacts Group National Center for Atmospheric Research, 2002.

F. Martin Ralph, Paul J. Neiman, David E. Kingsmill, P. Ola G. Persson, Allen B. White, Eric T. Strem, Edmund D. Andrews, and Ronald C. Antweiler. The impact of a prominent rain shadow on flooding in California's Santa Cruz mountains: A CALJET case study and sensitivity to the ENSO cycle. Journal of Hydrometeorology, 4(6):1243-1264, 2003.

Kelly T. Redmond and Roy W. Koch. Surface climate and streamflow variability in the western United States and their relationship to large-scale circulation indices. Water Resources Research, 27(9):2381- 2399, 1991.

Chester F. Ropelewski and Michael S. Halpert. North American precipitation and temperature patterns associated with the El Niño/Southern Oscillation (ENSO). Monthly Weather Review, 114(12):2352-2362, 1986.

T. Schonher and Sharon E. Nicholson. The relationship between California rainfall and ENSO events. Journal of Climate, 2(11):1258-1269, 1989.

Richard T. Sylves. Disasters and coastal states: A policy analysis of presidential declarations of disaster 1953-97. Technical report, University of Delaware Sea Grant College Program, 1998.

Richard T. Sylves and William L. Waugh, Jr., editors. Disaster management in the U.S. and Canada : the politics, policymaking, administration, and analysis of emergency management. Charles C. Thomas, Springfield, Illinois, 1996.

David W. J. Thompson and John M. Wallace. Regional climate impacts of the northern hemisphere annular mode. Science, 293(85):85-89, 2001.

U.S. Army Engineer Institute for Water Resources U.S. Army Corps of Engineers. Flood risk management, value to the nation. Technical report, 2009.

Klaus Wolter and Michael S. Timlin. Measuring the strength of ENSO events: How does 1997/98 rank? Weather, 53(9):315-324, 1998.

Atmospheric Rivers Drive Flood Damages in the Western US

Thomas W. Corringham, Alexander Gershunov, and Daniel R. Cayan

Abstract

This paper quantifies the economic impacts of flooding due to atmospheric river (AR) events in the western United States from 1978 to 2007, using National Flood Insurance Program (NFIP) claims and loss data. Comparable to hurricanes and tropical storms in the eastern United States in their discrete and episodic nature, ARs are responsible for much of the intra-seasonal and inter-annual variability in west coast hydrology. Analyses of the NFIP data confirm that AR-related floods cause significant economic damages and constitute the primary source of insurance claims and insured flood losses in the western coastal states. The spatial and temporal structure of damages can be represented as a function of integrated vapor transport (IVT) and antecedent hydrologic conditions. These results can be used to inform policies to mitigate flood losses and respond to future flood disaster scenarios.

1 Introduction

Atmospheric rivers are temporally ephemeral yet vertically stable filamentary features in the lower troposphere that convey large quantities of moisture from the tropics to higher latitudes and cause extreme precipitation events on west coasts of major landmasses including North America due to orographic lift over mountainous topography (Zhu and Newell 1998, Gershunov *et al*. 2017). Atmospheric rivers are an important source of intra-seasonal and inter-annual variations in precipitation, streamflow, and hydrologic flood events. ARs tend to be warm storms,

producing more rain than snow compared to other winter storms, and AR precipitation is strongly orographic. These phenomena have received increasing attention in the climate literature (Dettinger *et al*., 2011; Dettinger, 2015; Ralph and Dettinger, 2011) and are beginning to receive attention in the popular press (*e.g.* Kasler *et al.* 2017), but remain largely unstudied by the economics community.

There is a growing awareness that atmospheric rivers are responsible for a wide range of social and economic impacts in western coastal states. Dettinger (2011, 2015) notes that the frequency and magnitude of AR events are responsible for drought duration and intensity, and for the frequency and severity of extreme flood events. ARs have been identified as the primary source of hydrologic flooding in the western US (Barth *et al.* 2017, Dettinger and Ingram 2013, Neiman *et al.* 2011, 2013, Ralph *et al.* 2006). But not all ARs cause hydrologic flooding, and not all hydrologic floods are economically damaging (Hoyt and Langbein 1955, Pielke and Downton 2000, Pielke *et al.* 2002).

The costs of several extreme AR events have been estimated: for example, the New Year's flood of 1997 caused by AR(s) making landfall over central and northern California is estimated to have caused over $1.6b in damages (Perry, 2005). A series of papers by teams including climatologists and social scientists describe a 1-in-1000-year AR event, the "ARkStorm" scenario, including cost estimates (*e.g.* Porter *et al.* 2010). Yet, to date there have been no systematic economic analyses of AR events in recent history. In this paper we provide the first analysis of flood damages caused by AR events in the western United States using flood insurance data from the NFIP, combined with cost data from the National Weather Service (NWS).

The impacts vary seasonally, by location, and with respect to the intensity of the event and antecedent hydrologic conditions. In our 30-year time sample, 48% of the 1074 AR events, as identified by Gershunov *et al.* 2017, cause insured losses. The average AR event causes approximately $700,000 in NFIP insured losses. From this we estimate the total impacts of each AR event at approximately $20m, as explained below. The most damaging AR events in our sample cause $70m to $80m in insured losses, which translate into billion-dollar events in terms of total impacts.

There is a great practical need to determine which ARs are most likely to cause significant damages. Where have the most damaging ARs made landfall? What was the directionality or orientation of the most damaging ARs? What were the antecedent hydrologic conditions associated with the most damaging ARs? We approach this problem by estimating the probability and magnitude of flood damages as measured by NFIP insured losses, conditioned on insured exposure to risk, AR intensity, and antecedent hydrologic conditions.

After presenting summary statistics of AR impacts by day and location and by event, we describe the spatial and temporal characteristics of insured losses caused by AR events. We present a diagnostic vector field canonical correlation analysis linking the field of integrated vapor transport (IVT) over the North Pacific to NFIP losses in the western United States, in order to investigate how AR position and direction affect flood damage. Finally, we describe results from a model of damages as a function of location, vulnerability, AR characteristics, and antecedent hydrologic conditions.

2 Data Sources

2.1 Economic Data

Loss data were obtained from the NFIP. The data comprise daily claims from 1978 to 2007, and contain a single record for each claim, listing the date of loss, the location of the claim to the nearest NFIP community (city, typically, or county remainder), and the total insured loss, including damage to the structure and contents. To measure vulnerability or risk exposure, we use NFIP data on annual number of policies, premium payments and coverage in force by NFIP community. Dollar loss figures are adjusted throughout this analysis for inflation to 2017-USD using annual GDP deflators obtained from the Bureau of Economic Analysis (BEA 2018).

Previous analyses of the NFIP (Pasterick 1998, Michel-Kerjan 2010, Horn and Brown 2016) highlight the effects of population growth, increased development in flood-prone areas, and critical failures in government policy as factors that have exacerbated flood risk in the United States. In spite of increased mitigation efforts to discourage development in flood prone areas and to buy back properties that suffer repeated losses, vulnerability to flood risk continues to increase as coastal populations and the economic value of structures increase (Changnon *et al.* 2000). A comparison of 1983-2003 annual NFIP losses to a National Weather Service (NWS) compilation of economic impacts of flooding (Pielke *et al.* 2002) shows that, in the 11 western states, NFIP insured losses account for roughly one thirtieth of total damages as estimated by the NWS (Figure 3.1). The Pearson correlation between the two series is high at 0.8, indicating that NFIP losses explain 64 percent of the total economic impacts of flood events.

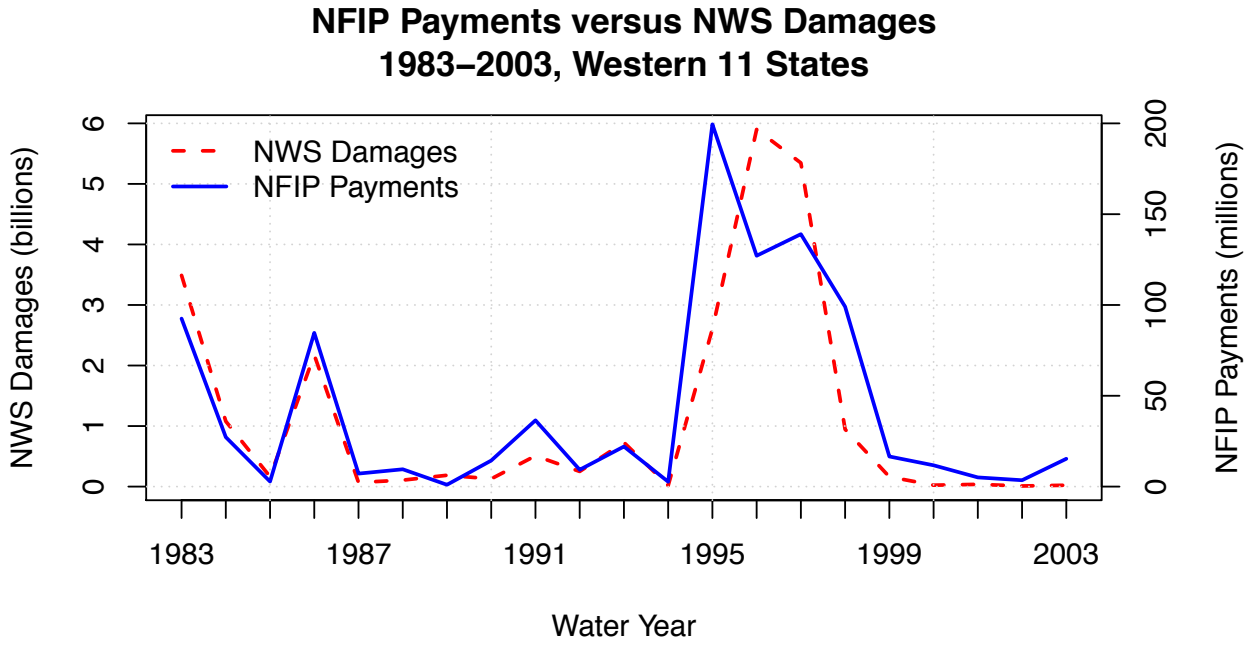

Figure 3.1: NFIP payments versus NWS damages. Annual aggregates of inflation-adjusted NWS damage estimates (dashed red line) and NFIP insured losses (solid blue line) reveal strong coherence (correlation = 0.8). Discrepancies in years 1995 through 1998 may be due to a significant NFIP "Cover America" campaign in 1995 followed by policyholders dropping their contracts in the following years.

Although the NFIP data have several attractive features, they also suffer from significant limitations. Participation rates are surprisingly low in the western United States, even in relatively high risk areas, so the number of claims and insured losses are an imperfect measure of total impacts. Several biases are expected. Floods in unexpected areas will be underrepresented. The NFIP program covers only residential property, so floods that cause disproportionate damage to agriculture, infrastructure, and industrial plants will be down-weighted in this analysis. Older properties receive subsidies and are likely overrepresented in the portfolio of risks. This is one of many distortions in the NFIP. The market for insurance is not a free market and does not behave like one (Kunreuther 1998).

These caveats aside, the NFIP data is daily resolved and spatially specific (at the level of NFIP community), so they provide a useful source with which to assess the economic impacts of flood events associated with atmospheric rivers and extreme hydrologic events more generally.

2.2 Atmospheric Rivers

Atmospheric river data were obtained from Gershunov *et al*. 2017 (G17) who present an AR detection methodology through which they compile a comprehensive catalog of AR events (SIO-R1) over 70 years using National Center of Environmental Prediction-National Center for Atmospheric Research reanalysis. Their detection methodology identifies the ARs that make landfall along the Pacific coast of North America over a 2.5 degree coastal grid. ARs identified are those events whose 6-hourly average integrated vapor transport (IVT) exceeds 250 kg/m/s, along with exceeding prescribed specific humidity and conforming to certain geometric requirements. In addition to time and place of AR occurrences, G17 also provide integrated water vapor (IWV) and the zonal and meridional components of IVT and wind at 850 hPa over a 2.5 degree grid of the north Pacific and the western United States at a 6-hourly time scale. For our study, we aggregate these data to daily resolution, using the 30 years (1978-2007) of data for which we have corresponding NFIP data.

In the SIO-R1 data, there are 1174 events in our 1978-2007 sample. The durations of events in our sample range from 6 hours to 12.5 days, with median duration of 30 hours, and mean duration of 40 hours. We consider events making landfall from 27.5N to 47.5N, that is, over nine 2.5 degree latitude bands. During the course of a multi-day event, an AR may make landfall at more than one latitude band. In our sample we observe events making landfall at one to nine

separate 2.5 degree latitude bands. The mean number of land-falling latitude bands was 2.65. The median and modal number of latitude bands was two.

2.3 Hydrologic Data

To assess how flood damage is affected by antecedent land-surface hydrology, soil moisture, and snow pack, we use model data from the Variable Infiltration Capacity (VIC) hydrology model (Liang *et al.* 1994). We aggregate 1/8 degree resolution data to the county level. Key variables considered in our models include daily precipitation (mm/day), runoff (mm/day), soil moisture (mm), snow water equivalence (mm), and snow depth (mm/day).

3 Methods and Results

3.1 Economic Impact of Atmospheric Rivers

For our analysis of the impacts of ARs on insured losses we begin with a naïve approach in which we aggregate NFIP loss data to the same 2.5 degree grid over which IVT is aggregated, over seven coastal grid cells from 32.5N to 47.5N. To assess the impacts of land-falling AR events at each of the seven coastal grid points, we calculate mean number of claims, claims paid, and insured losses over the extended cool season months of October through March (ONDJFM) with and without AR activity, on the same day, at the same grid cell. Later we consider a broader spatial and temporal classification of AR activity. We choose to focus on ONDJFM in this analysis as the vast majority of losses and AR events in our sample occured during these months. Hence our data consist of 5,356 days (30 years of ONDJFM) by 7 grid cells for a total of 37,492 cell-days.

The cost of each AR event varied with the location and intensity of the event. We conducted several analyses to quantify the economic impact.

3.1.1 Difference in Daily Losses with and Without AR Activity

Table 3.1 presents a comparison of claims, claims paid, and insured losses with and without AR activity (max 6-hourly IVT per day greater than 250 kg/m/s). We observe that insured losses increased from $6,205 per cell-day on the 34,508 cell-days with no AR activity to $130,982 per cell-day on the 2,984 cell-days with AR activity ($p = 1.2 \times 10^{-6}$ on a Welch two-sided *t*-test).

An obvious question is how AR intensity affects losses. To examine this we divide the AR events into quartiles conditional on AR activity. During AR events in the highest quartile (max 6-hourly IVT per day > 530 kg/m/s), mean insured losses per cell day increased to $403,018, a 65-fold increase relative to cell-days with no AR activity ($p = 2.1 \times 10^{-5}$). In this analysis only losses that occur on the same day as AR landfall are included, not on days one or more days after landfall. Later we show that peak losses occur the day after landfall, so the large and significant results presented here are conservative measures of AR impacts.

Table 3.1: Average ONDJFM claims and losses per grid-cell-day

	Overall	max IVT < 250 (a)	max IVT > 250 (b)	max IVT > 345 (b)	max IVT > 424 (b)	max IVT > 530 (b)
Claims	1.13	0.52	8.24	10.25	14.57	22.45
Claims Paid	0.83	0.35	6.39	8.01	11.46	17.95
Loss (USD)	16,136	6,205	130,982	164,908	240,879	403,018
Number of Grid-Cell-Days	37,492	34,508	2,984	2,245	1,497	746
Fold Change						
Claims	2.17	1	15.85	19.71	28.02	43.17
Claims Paid	2.37	1	18.26	22.89	32.74	51.29
Loss (USD)	2.6	1	21.11	26.58	38.82	64.95

(a) max IVT < 250 indicates no atmospheric river activity
(b) *t*-statistics on differences in means > 4 throughout (versus days with no AR activity)

3.1.2 Difference in Daily Losses by Crossing Latitude

Next we perform the same analysis by latitude. Results are presented in Table 3.2. Of interest, in the 37.5N grid cell, we observe the greatest increase in losses during AR events relative to those when no ARs are present, a 149-fold increase in losses. AR events are known to cause significant damages along the Russian River in northern California (Ralph *et al.*, 2006). The lower reach of the Russian River falls into our 37.5 degree grid cell, as does the Bay Area south to Monterey.

The results in other latitude bands were significant but less strong, ranging from a 15-fold increase at 40N to a 140-fold increase at 35N. Results below (Section 3.6: Damage Function) indicate that the variation in AR effects by latitude was due primarily to two factors: differences

in vulnerability at different latitudes, and in intensity of AR events. Interestingly, while G17 find land-falling AR events of maximum intensity at 40N, at this latitude we see the lowest effect on losses. This appears to be due to the low population density in this coastal grid cell rather than the intensity of AR events.

We also find a relatively low effect, though still significant, of AR activity at 32.5N in southern California. This may be due to the low number of days with IVT > 530 kg/m/s at this grid cell (34 days over the 5356 day period). It may also be due to the fact that land-falling ARs at this latitude had a strong southerly component, indicating that the IVT intensity at 30N may have been more strongly associated with losses at 32.5N. These results lead us to assess below whether IVT at various temporal and spatial lags could be more closely tied to increases in losses than same-day same-location IVT.

Table 3.2: Average insured loss by ONDJFM day by latitude band by AR intensity

	47.5 N	45 N	42.5 N	40 N	37.5 N	35 N	32.5 N
Fold change no AR	1	1	1	1	1	1	1
Fold change all days	1.5	3	5.1	1.3	4.4	2.9	2.3
Fold change max IVT > 250	7.3	20.4	44.4	4.3	40.9	33	28.6
Fold change max IVT > 530	25.9	65.8	129.2	15.3	149.2	140.4	33.0
Loss no AR (USD)	13861	2819	180	5768	12676	2501	5579
Loss all days (USD)	20764	8497	920	7464	55507	7159	12640
Loss max IVT > 250 (USD)	100854	57523	7984	24570	517975	82465	159314
Loss max IVT > 530 (USD)	359288	185452	23260	88151	1890693	351236	184132
n days no AR	4931	4800	4848	4873	4902	5044	5110
n days all days	5356	5356	5356	5356	5356	5356	5356
n days max IVT > 250	425	556	508	483	454	312	246
n days max IVT > 530	106	168	162	118	101	57	34

3.2 Proportion of Losses Due to AR Activity

We have shown that AR events significantly increased insured flood losses throughout the coastal western states. A related question concerns the fraction of total insured losses in any given location due to atmospheric rivers. We would expect that not all flooding in the western US is due to atmospheric rivers. Indeed this is true in our sample, particularly in leeward areas protected from the intense winds and precipitation associated with AR events. However, as shown in Table 3.3 and Figure 3.2, we find that atmospheric rivers were responsible for a substantial proportion of total losses. Over the 11 western states, the proportion of losses that occurred on days with any AR activity (IVT > 250 kg/m/s) at latitude bands from 27.5N to 47.5N (2,424 days, or 26.48 percent of our 10,681 day sample) accounted for 83.91 percent of insured losses. We note that this remarkably high figure is likely a conservative estimate, given that AR events were associated with elevated losses for several days after the end of the event as identified by the SIO-R1 detection methodology, and as shown below.

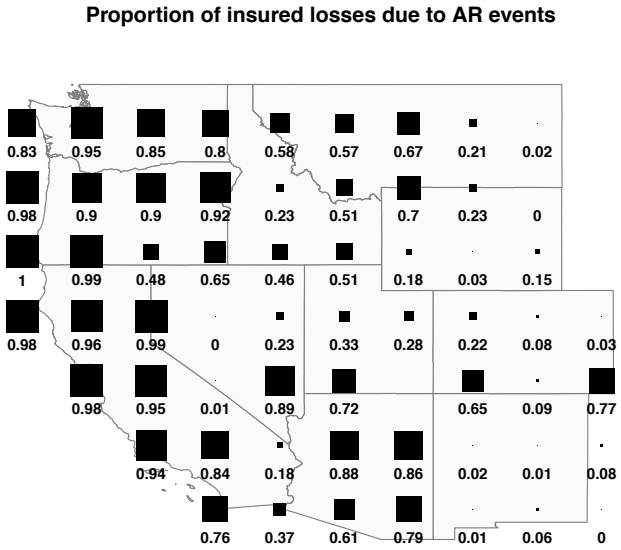

Figure 3.2. Proportion of insured losses due to AR events: effects of AR activity (IVT > 250 kg/m/s over nine coastal grid cells from 27.5N to 47.5N) over a 2.5 degree grid. Proportions were especially high in northern California and western Oregon. Lower proportions are seen in the interior western US, as expected.

The spatial pattern of losses associated with AR activity is shown in Figure 3.2. Remarkably high proportions of losses were associated with AR activity as far east as 100W, including much of Arizona, Idaho and western Montana. Losses in Arizona were due to ARs making landfall in Baja California; losses in Idaho and Montana appear to have been a result of inland penetration of ARs through the Columbia River Valley. In a sense, these are liberal estimates of proportions of losses associated with AR activity, since they aggregate over all days with relatively mild AR conditions (IVT > 250 kg/m/s) and over 11 crossing latitude bands, extending from Baja California Sur to Washington.

Recreating this figure to show total losses for a given latitude band associated with AR conditions within that particular latitude band, would reveal lower proportions of losses associated with AR conditions, as expected. However, many AR events are not limited to a single latitude band but move over a wide spatial extent over the duration of the event. Also, damages associated with each event are distributed over a much wider spatial extent than the crossing latitudes. For these reasons we argue that the presented measures of proportions of damages associated with AR events by location are reasonable.

In Table 3.3, we report the fractions of total losses associated with AR activity for the 20 counties with the greatest losses over our time period (these 20 counties accounted for roughly two thirds of total losses in our sample of 414 counties). Proportions were as high as 0.997 in Washoe County Nevada, which contains Reno Nevada on the Truckee river, and 0.98 for Marin and Sonoma counties in California. Sonoma County had the highest losses of the 414 western counties over our sample period, and among the highest losses per policy of the western states. Again, these are liberal estimates as they aggregate over all 11 crossing latitude bands. However, limiting the crossing latitude bands to those which significantly affect losses at each location does not appear to weaken the results.

Table 3.3: Proportion of losses caused by AR events by top counties

	County	State	Insured Losses (millions)	AR Insured Losses ($ millions)	AR Proportion	Claims	Estimated Damages ($ billions)
1	Sonoma	CA	159.490	158.421	0.993	6089	4.478
2	Los Angeles	CA	91.276	76.798	0.841	7443	2.563
3	Marin	CA	69.063	68.218	0.988	2807	1.939
4	Sacramento	CA	52.160	51.052	0.979	3273	1.464
5	Napa	CA	42.327	42.215	0.997	1295	1.188
6	Monterey	CA	41.903	41.592	0.993	1192	1.177
7	Lewis	WA	41.722	40.439	0.970	1080	1.171
8	King	WA	39.742	38.807	0.977	1845	1.116
9	Washoe	NV	39.032	38.917	0.997	572	1.096
10	Clackamas	OR	26.733	25.825	0.966	606	0.751
11	Snohomish	WA	26.519	25.940	0.978	1146	0.745
12	Placer	CA	25.586	25.228	0.986	534	0.718
13	Orange	CA	24.624	21.812	0.886	3169	0.691
14	Santa Clara	CA	23.541	22.843	0.970	1253	0.661
15	Maricopa	AZ	20.847	13.716	0.658	1829	0.585

In considering the top 20 counties in terms of losses, we observe lower proportions of total damages caused by AR events in the Pacific Northwest (Lewis Washington, Clackamas Oregon, Cowlitz Washington) and the interior southwest (Maricopa Arizona). In the northwestern U.S. this may be due to the fact that annual precipitation levels were generally higher than in the southwestern U.S., and there may have been more slow rise flooding. In Arizona it may have been due to non-AR monsoon flooding in the late summer flood season there. We also observe a lower proportion of losses due to AR events in southern California. It is not clear if this is due to significant non-AR flood events or to the high population densities, coverage levels, and overall risk exposure. It may be that areas with especially high population densities are more susceptible to idiosyncratic flooding not related to AR events; or perhaps southern California is more susceptible to flash flooding and hillside mudslides caused by storms other than AR events. A final possibility is that events in certain regions are longer in duration and losses fall on days between

AR events, but are still, in a sense, caused by the ARs. Further work is required to untangle the possibilities.

3.3 Accounting for Spatial and Temporal Lags

We have shown above that, as an average over the western U.S., AR events increase same-day same-location losses by a factor of 21, and that strong AR events (IVT > 530) increase same-day same-location losses by a factor of 64. However, G17 report that precipitation levels are still elevated the day after AR landfall. They also show that many ARs have a strong southerly component, so we would expect heaviest precipitation and peak damages to occur to the north of AR landfall, often on the few days following elevated IVT.

Time series of daily claims versus AR landfalls by latitude over the seven latitude bands corresponding to the western states (Figure 3.3) reveal several interesting features. We present two years (ONDJFM) of interest: 1995/96 and 1997/98. In blue we show AR events with IVT > 250. In orange we overlay daily claims on a log scale. One pattern that is evident in these two time series plots reinforces findings in earlier work: there was a clear spatial progression of AR activity from the Pacific Northwest to southern California over the course of the extended cool season, with peak AR activity occurring in the northern latitudes in October through December, and peak activity in the southern latitudes from January through March. This seasonality corresponded to a similar seasonality in insured losses.

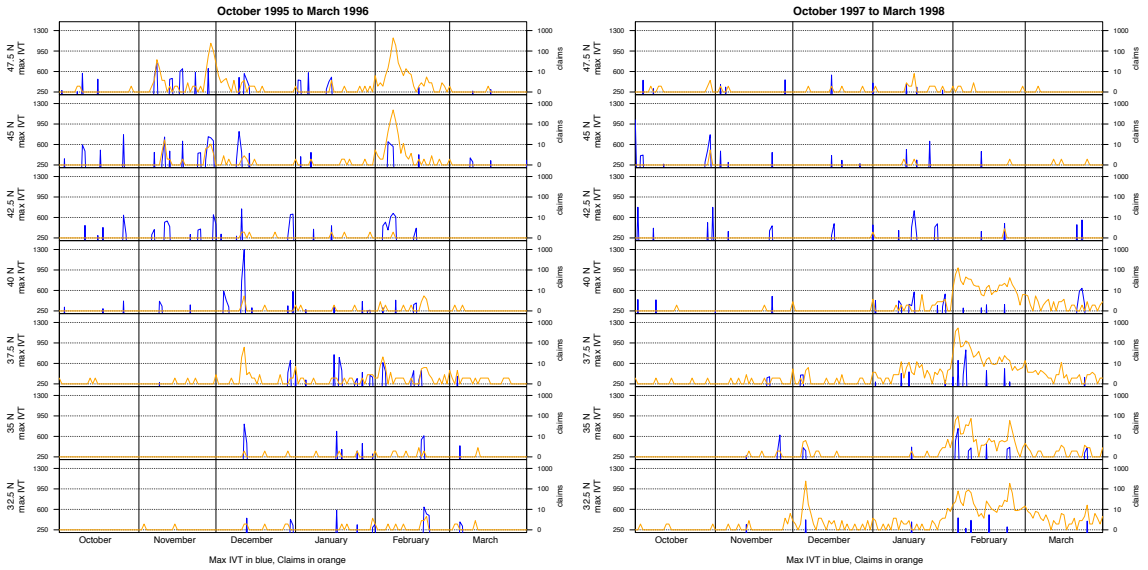

Figure 3.3: Time series of claims versus AR activity by latitude band, 1995/96 and 1997/98. AR events (daily maximum IVT > 250 kg/m/s) shown in blue on a linear scale over land-falling latitude bands 32.5N to 47.5N, with corresponding daily number of NFIP claims shown in orange on a logarithmic scale.

In 1995/96, a moderate La Niña year, we observe significant damages in the Pacific Northwest in November and, somewhat uncharacteristically for the region, also in February. For the February losses we see extreme losses in the 47.5N band with no corresponding AR activity. In the 45N band however there was AR landfalling activity, indicating that the losses at 47.5N were indeed associated with a land-falling atmospheric river event, where landfall occurred south of observed losses.

In the historic 1997/98 El Niño year, record losses were observed from 32.5N to 40N in the months of January through March, concentrated in the record-loss month of February 1998. Coincident with these extreme losses we observe several land-falling AR events as identified by the SIO-R1 detection methodology.

3.4 Temporal Variation

3.4.1 Temporal Lags

In terms of temporal effects we find that IVT was most strongly correlated with next-day losses. AR activity leading losses makes sense from a mechanistic perspective as precipitation caused by AR landfalls may take a day to circulate through river systems to cause losses. These results are demonstrated in Figure 3.4, in which trimmed means of insured losses are plotted by event against dates preceding and following landfall.

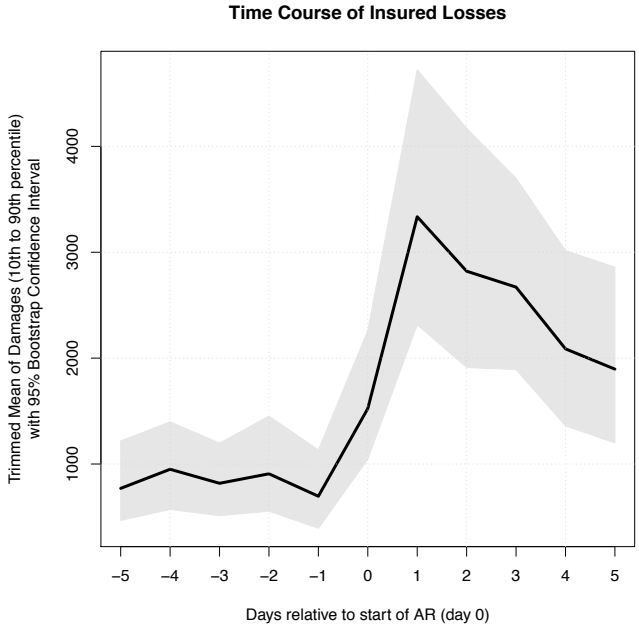

Figure 3.4: Time course of insured losses. Trimmed mean of NFIP insured losses per day of event, from 5 days ahead to 5 days post-landfall. 95% confidence intervals were bootstrapped with 1000 replicates. An 80% increase in damages relative to baseline is observed on the day of landfall; a 300% increase is seen on the day after landfall. A trimmed mean (mean of values from the 10th to 90th percentile) was used to exclude outliers which masked the key temporal pattern.

3.4.2 Top Events

Table 3.4 displays the 14 events which caused over $20m in insured losses. These 14 events, spanning 82 days, accounted for 68.1 percent of total insured losses over the 30 year time period. This highlights the highly episodic nature of extreme flooding in the western United States. The length of each highly damaging AR event ranged from 3 to 11 days. We note that maximum IVT values were very high for the majority of these events. The geographic distribution was relatively wide with highly damaging AR events making initial landfall from Baja California Norte to Washington State. Estimates of total losses, using our rough metric of thirty times total insured losses rose as high as $3.5b. These estimates at the top end are likely overestimates, but reflect the order of magnitude of these events, in the billion dollar range.

Table 3.4: Most damaging AR events (insured losses over $20m)

Start Date	Number of Days	Claims	Insured Losses ($ millions)	Estimated Damage ($ billions)	Crossing Latitude	Crossing Region	Max IVT
1/4/95	11	4725	125.8	3.531	32.5	S. California	922.47
12/29/05	5	2553	115.3	3.237	40	N. California	780.84
12/29/96	8	3407	104.6	2.936	35	Central Coast	1215.73
2/5/96	4	2695	99.3	2.787	45	N. Oregon	684.56
2/15/86	5	2048	66.6	1.871	47.5	Washington	825.94
3/7/95	5	2343	58.7	1.649	42.5	S. Oregon	883.79
2/1/98	3	2417	46.7	1.312	37.5	Bay Area	751.30
11/1/06	7	1145	35.3	0.991	40	N. California	996.58
1/25/83	5	1545	34.9	0.979	37.5	Bay Area	968.56
2/25/83	7	1832	30.0	0.841	37.5	Bay Area	613.87
2/12/80	9	2059	28.5	0.799	30	Baja Norte	677.02
1/3/82	3	1422	28.1	0.790	40	N. California	480.87
2/11/86	5	848	23.9	0.670	40	N. California	859.92
11/21/90	5	939	23.3	0.654	47.5	Washington	899.02

3.4.3 Top Days

Reinforcing the per-event results presented in Table 3.4, in Figure 3.5 we plot all days with insured losses greater than $1m over the entire western US. We see the vast majority of high loss days occurred during AR events. Several of these days were ones that occurred within the top events described in 3.4.2. The damages are plotted on a logarithmic scale, which enhances the visibility of the less damaging events, but diminishes that of the most significant events, which are highly infrequent and episodic. Over the 1977-2007 sample there were only 24 days, comprising 13 separate events, on which insured losses exceeded $10m. These 24 days accounted for 53.1 percent of total insured losses, and of them only one occurred in the absence of AR conditions on the day of or the day preceding damages. Understanding these extreme events is the key to understanding flood damages in the western US, and virtually all of these extreme loss events were caused by atmospheric rivers.

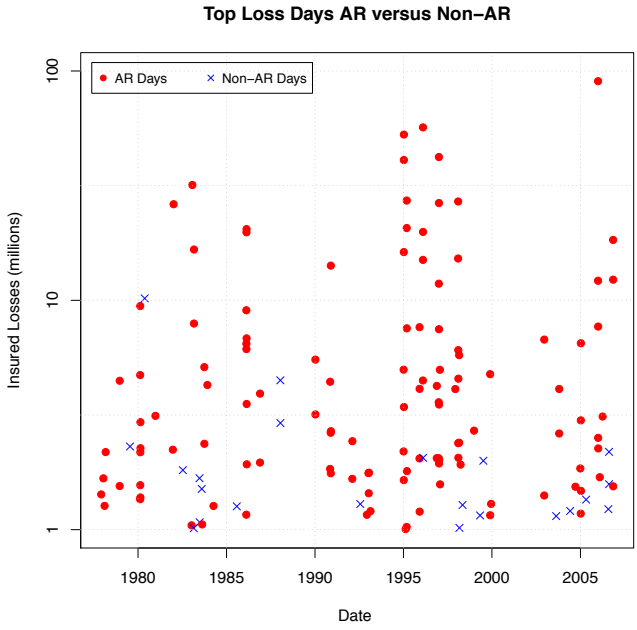

Figure 3.5: Top loss days, AR versus non-AR. Daily NFIP insured losses over $1m from 1978 to 2007; AR days are red dots, non-AR days are blue crosses. 130 of 142 days with losses over $1m and 23 of 24 days with losses over $10m occurred during AR events.

3.5 Spatial Variation

As discussed above, there were clear differences in AR impacts by location, by land-falling latitude in particular. In Figure 3.6, we color each county in the western US according to the AR latitude band associated with the greatest losses for that county.

Of interest we note that ARs that made landfall in Baja California at 27.5N produced losses in Arizona, New Mexico, and southern Nevada, consistent with similar observations in the hydro-climatology with respect to inland penetration (G17, Rutz *et al*. 2014). ARs that made landfall at 30N, in Baja California Norte, were most significantly connected to losses in Arizona, New Mexico, southern Nevada, southern California, and, somewhat surprisingly, as far north as the Bay

Area and the San Joaquin Valley. ARs making landfall 35N and 37.5N were most strongly connected to losses in central and northern California. ARs making landfall to the south at 32.5N and to the north at 40N had less of an effect. ARs making landfall at 42.5N and 45N had strong connections to losses in the Pacific Northwest, where deep inland penetration is also notable. ARs making landfall at 47.5N had little effect on losses in the US though may have caused damages in British Columbia, an area for which we have no loss data.

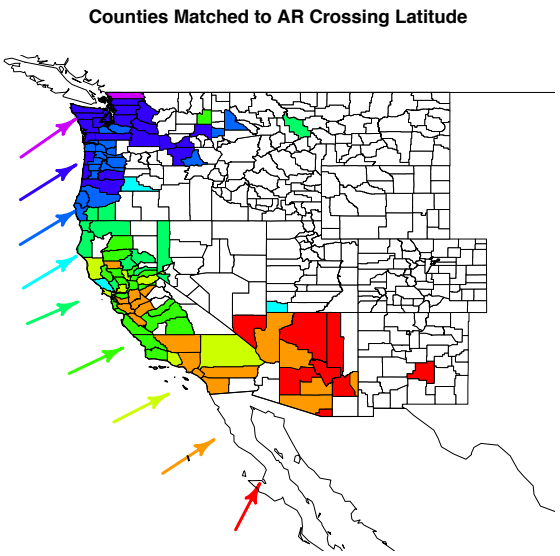

Figure 3.6: Affected counties matched to crossing latitude. Insured losses were summed by AR day by crossing latitude. Counties are colored to match AR crossing latitudes with greatest aggregate damages. Orientation of arrows indicate the mean directionality of IVT at landfall.

3.5.1 Spatial Composites and Effects of Orientation of AR Wind Vector Field

Supporting the results just described, in Figure 3.7 we present spatial composites of losses over the west coast associated with AR events that make landfall at 32.5, 37.5 and 47.5 degrees

north. In the left panel we plot differences in mean insured losses on days with AR activity at the specified latitude band versus days without such AR activity, with a logarithmic color scale. In the right panel, we present the relationship between the orientation of winds associated with the IVT (the vector wind at 850 hPa from G17) and insured losses.

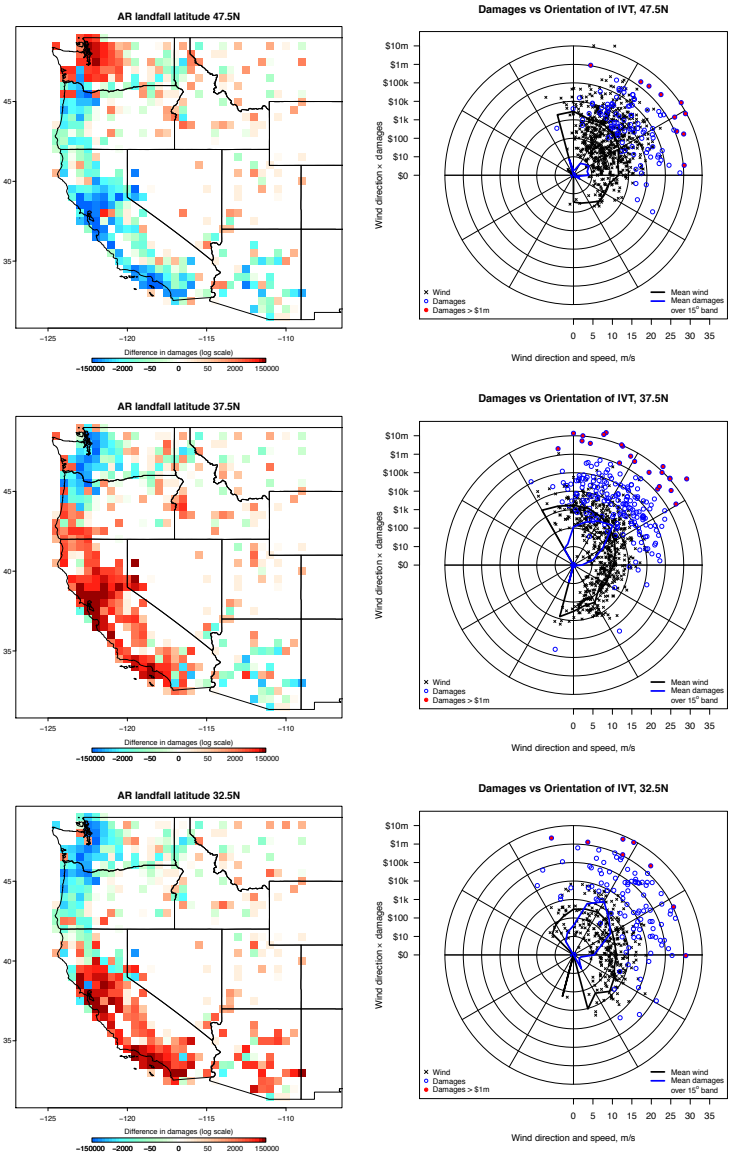

Figure 3.7: Spatial composites and orientation of AR wind field. Aggregate differences in insured losses on AR days versus non-AR days, by crossing latitude (here at 47.5N, 37.5N, and 32.5N from top to bottom), on a bi-log scale, are plotted in the first column. The second column plots orientation effects at the same latitudes. Azimuths indicate mean daily 850 hPa wind directions. Here, direction is defined as the direction the wind is blowing toward, where 0 is wind blowing to the east, 90 is wind blowing to the north, -90 is wind blowing to the south. For each AR day a black cross with radial distance equal to wind speed and a blue circle with radial distance equal to the logarithm of insured loss are plotted. Losses over $1m are colored red for emphasis. The solid lines plot mean wind speeds and losses aggregated over 15 degree sectors, in black and blue respectively.

In the spatial composites, at 32.5N we see increased loss activity over southern and central California, and some loss activity in the interior southwest, Arizona in particular. While ARs that made landfall further north were blocked from causing damages inland, by the Sierra Nevada mountain range for example, those to the south, making landfall in Baja California face no such topographic obstacles and caused damaging floods further inland. The increased losses in central and northern California associated with AR events that made landfall at 32.5N are in line with observations that the strongest AR events in California exhibit a southeasterly flow. This observation is further borne out in the orientation figure.

At 32.5N, wind directions associated with AR events ranged from -100 to 120 degrees. Losses were also widely dispersed by wind direction, though the directions with most losses were concentrated between 0 and 110 degrees, with eight events with insured losses within the 32.5N latitude band in excess of $1m. Mean losses were even more concentrated from 30 to 75 degrees. We note that mean losses can be low in areas with high loss events if there are many AR days with zero damages in that 15 degree direction band.

At 37.5N in the spatial composite we see increased losses extending northward as far as southwestern Oregon, and a weakening of losses in Arizona and the southwest. At this point the southwest is protected from AR moisture flow and enhanced precipitation by the Sierra Nevada range. Interestingly we see enhanced damages in western Nevada in the Reno area associated with lee-side spillover events causing extreme flow on the Truckee River with headwaters at Lake Tahoe in the Sierra Nevada range. Unsurprisingly we see highly enhanced damages in areas of relatively dense, high-value development surrounding San Francisco Bay, including Sonoma County and the Russian River to the north.

At 37.5N there were more AR days and a greater number of loss days than at 32.5N. AR wind directions were widely dispersed from -115 to 120 degrees. Losses were concentrated between 30 to 90 degrees, with 21 days with losses within the direction band over $1m, of which nine days caused insured losses over $10m, roughly equivalent to $300m in total damages. Damages were much higher at 37.5N compared to 32.5N as the latitude band includes the Bay Area and the Russian River to the north. As at 32.5N, greater losses occurred when the winds had more of a southeasterly component. This is likely due to the orientation of the coastline and the orientation of the Sierra Nevada and Transverse ranges.

As AR events made landfall at 47.5N, damages were concentrated in western Washington. A noticeable gap in losses is observed in the Olympic peninsula where population density and exposure are low. We speculate that, given the general southerly flow of ARs, events making landfall at 47.5N are likely to be associated with increased flood damages throughout coastal British Columbia, although we do not have loss data for the Canadian provinces.

In terms of the orientation of IVT wind flow, at 47.5N AR winds were more concentrated. The overall directionality ranged from -90 to 110 degrees as at lower latitudes, but far more days were concentrated in the 0 to 90 degree range. Losses likewise were concentrated in the same degree range. Mean losses reveal a strong westerly component. This again may be due to the orientation of the coastline, of the Cascades, and perhaps due to the fact that the Seattle metropolitan area is protected from AR events of a more southerly flavor by the Olympic mountain range.

Further results, for all crossing latitudes are presented in the Appendix in Figure 3.11. Results are consistent with those presented here. Spatial composites are generated for crossing

latitudes from 22.5N to 50N. Enhanced losses in the western states are observed for crossing latitudes ranging from 25N to 47.5N. We note that one limitation of the present orientation figures presented is that, unlike the spatial composite maps, the losses shown are those within the same latitude band as that of AR landfall. Based on the spatial composites we presume that the northward bias in losses vs wind directionality observed for ARs that make landfall in California would be enhanced if losses from higher latitude bands, or the whole west coast, were included in the figures.

3.5.2 Relating Pacific-North American IVT to Damages using CCA

Past work has linked seasonal variability and predictability in the frequency of heavy precipitation to sea surface temperature (SST) patterns, particularly associated with El Niño-Southern Oscillation and the Pacific Decadal Oscillation. Gershunov and Cayan (2003) examined predictive linkages between Pacific SST and conterminous U.S. heavy precipitation using canonical correlation analysis (CCA), which, in its diagnostic application, identifies temporally coupled patterns in two fields of variables. Land-falling ARs, which transport moisture evaporated from the ocean surface often produce heavy precipitation over rising terrain (G17). In turn it can be expected that economically damaging flooding will respond to IVT across the Pacific and along the coast in particular. To elucidate the association of Pacific IVT and associated flood damage over the western United States, we employ CCA to examine the principal patterns involved.

Though our focus is on the ONDJFM months during which the bulk of AR activity and insured flood damages occured, we apply CCA to the entire time domain, allowing the data and the method to identify peak periods of activity. Following G17 we apply directional CCA (García-Bustamante *et al.*, 2012), given that IVT is a vector field. In performing directional CCA we resolve both the zonal, *u*, and meridional, *v*, components of IVT, coupling IVT vectors over the

tropical and north Pacific with losses over the same spatial field, including the western conterminous United States, Hawaii, and coastal cells in Alaska. G17 perform their CCA using IVT vectors at land-falling SIO-R1 grids. We perform our directional CCA over the entire spatial field of the data, allowing the data and the method to find the salient grid cells.

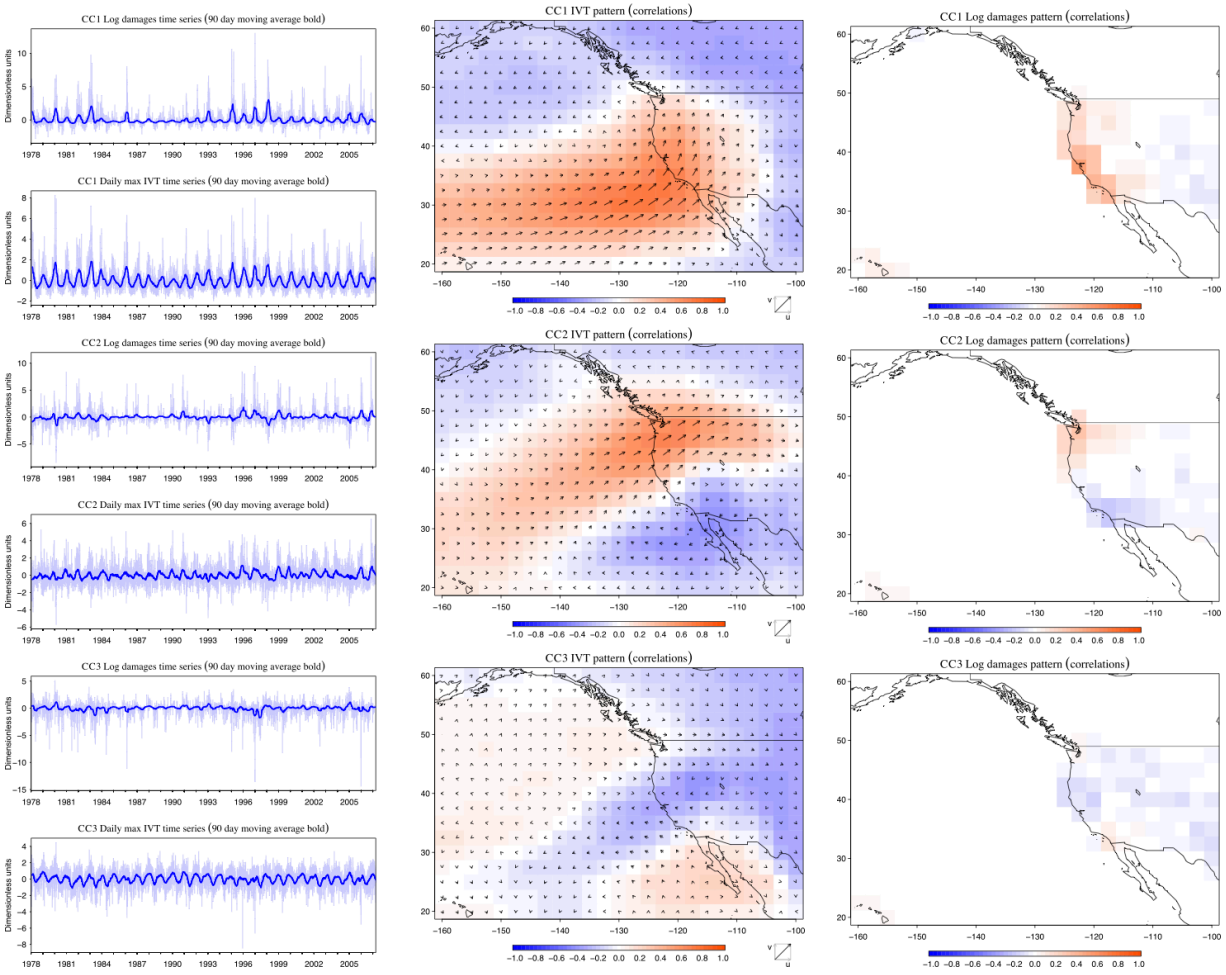

Figure 3.8: Canonical correlation analysis. (a) Leading canonical correlates (time series, with 90-day moving averages in bold to highlight the seasonal cycle and seasonal anomalies) and their associated spatial patterns expressed as correlations between the time series and their respective fields of variables: (b) *u* and *v* components of daily vector IVT as arrows with magnitudes in colors, and (c) insured loss magnitudes in colors. Maximum possible arrow length, shown to the right of the color scale in (b), is the square root of 2, corresponding to unit ($r = 1$) *u* and *v* components. (a-c) represent leading mode, (d-e) and (f-i) the second and third leading modes respectively.

Figure 3.8 shows the three leading coupled modes derived from CCA applied to IVT and the logarithm of same-day insured losses. CCA applied to IVT and next-day losses produced similar results. The sub-panels display the leading mode of optimally correlated pairs of IVT and loss time series (d-f) and the temporally coupled spatial patterns in the IVT vector field and insured losses (g-i). The spatial patterns are displayed as correlations of the corresponding canonical correlates (IVT or loss) with total IVT magnitude (colors) and IVT vectors.

The leading CCA mode represents the leading mean impact of AR activity on losses through the pair of spatial patterns in IVT and losses whose temporal correlation is optimal. The IVT field shows maximum IVT intensity off the coast of California, to the southwest of the peak losses identified in the loss field surrounding the Bay Area. The directionality of the vector field is also strongest in this area moving in a southwesterly direction, consistent with the heightened damages in the Bay Area. The overall pattern of directionality of the CC1 IVT field coupled with IVT intensity represents the classic example of strong North Pacific moisture transport from Hawaii to Central and Northern California, in the form of an AR. The associated spatial pattern of flood damage exhibits strong positive correlations that span the west coast of the United States from southern California to Washington. Though Hawaii and Alaska were not the foci of this analysis, we see moderate positive correlations in the first mode with Hawaii and a weak negative correlation with coastal Alaska. Weak negative correlations are also seen to the east of the coastal ranges, which is as expected as AR events do not penetrate to the interior of the continent. In addition to the strong positive correlations in the coastal grid cells, weak to moderate positive correlations are seen inland in the Pacific Northwest and the Southwest as AR events were able to penetrate the coastal ranges through the Columbia Gorge and through Baja California and the transverse ranges of Southern California.

The associated time series of damages and daily IVT (panels a,d,g) display a clear seasonal pattern. To the daily data we apply a 90-day moving average (bold line) which reveals years of high losses coupled with high AR activity. In panel a, in particular the strong El Niño years of 1983, 1998 stand out, associated with heavy losses in California, as does the moderate La Niña year of 1995, a very strong year for AR activity, during which heavy losses occurred in the Pacific Northwest.

A north-south dipole in losses and AR activity is clear in the second CCA mode, with IVT intensity and vector field strongest in the Pacific Northwest, but with significant IVT intensity evident in Baja and Southern California and the interior Southwest. The IVT vector field associated with the southern dipole is weaker and less spatially coherent than that associated with the northern dipole which is strong and penetrates inland from the coast along the northern border of the United States which also forms the northern limit of our loss data. The associated time series exhibits an ENSO connection, with high magnitude losses in the time series in opposite directions associated with significant El Niño and La Niña years.

The third CCA mode is less easy to interpret, capturing residual correlations remaining after the first two modes are accounted for. Weak positive correlations between IVT and loss fields are evident at the northern and southern boundaries of the loss data. IVT vector field patterns are weak and less coherent than in the first two modes. The overall patterns are likely modifying the first two modes. The daily time series exhibits the presence of a few significant outlying events that may be driving the overall pattern of correlations.

3.6 Damage Function: Exposure, IVT and Antecedent Soil Moisture

We have shown above that AR events were responsible for the vast majority of economically damaging floods in the western US. There is a clear connection between AR intensity (maximum IVT) and damages, and clear variation of damages by location, unsurprisingly, given the uneven spatial distribution of exposure, or number of flood insurance policies. Typical AR events spanned multiple days, had a southwest-to-northeast orientation, and resulted in peak losses in the days following landfall. However most AR events as identified by the SIO-R1 detection methodology are relatively weak, and only 47% of all AR events caused damages. In some areas with high overall losses, over 10% of losses occurred during non-AR events.

Thus, several questions remain which can be addressed by a quantitative modeling investigation. To what extent does exposure to risk interact with AR intensity to generate damages? In given locations does the orientation of IVT and wind flow significantly affect losses? How do antecedent hydrologic conditions, *e.g.* soil moisture and snowpack affect damages associated with ARs after controlling for intensity and orientation? How well do AR-specific variables (IVT, IWV) compare with traditional hydrologic variables in modeling insured losses? In this section we construct a set of models to address these questions.

We used a regularized linear model of flood damage losses using multiple regressors or explanatory variables. The regularized model reduced our set of regressors to the following: number of days in the AR event, number of latitude bands in the AR event, number of policies, zonal and meridional elements of wind, maximum wind speed, IVT, and IWV over the duration

of the event, and several VIC variables, *viz.* initial soil moisture, runoff, base flow, precipitation, snow depth, and snow water equivalent.

We further reduced the set of regressors to the following: number of policies, u and v components of wind, maximum wind speed, IVT, IWV, and initial soil moisture and snow depth. The number of days and latitude bands were captured by the number of policies, given our methodology of linking policy and hydrologic variables to each event (AR events occurring over multiple days and multiple latitude bands affect a larger number policyholders; see Appendix for further details). Moreover, the number of days and latitude bands were known only *ex post*, after the fact. In our analysis we chose to focus on explanatory variables with more of a predictive component. We removed base flow, runoff, precipitation and snow water equivalent on the first day, as these are correlated with IVT and IWV. We kept leading soil moisture and snow depth to capture the antecedent hydrologic conditions.

We pursued two modeling strategies. In the first simple method we regressed the logarithm of payments on our explanatory variables, and then through backwards iteration removed variables that were not significant or that did not contribute to the adjusted R^2 measure of model fit. In our second method we used a nested model, first using a logistic, or logit, regression to estimate the logarithm of the odds ratio that an event would cause positive losses (only 47 percent of events caused positive damages in this sample), and then a log-linear regression model to estimate damages conditional on damages being greater than zero. All regressors were scaled to mean zero and standard deviation one. We report the results in Tables 3.5 through 3.7.

Table 3.5 Full regression results

Variable	Loss	Logit(Loss > 0)	Loss | Loss > 0
Intercept	2.283***	-0.152*	4.43***
	(0.058)	(0.076)	(0.05)
Policies	0.509***	0.619***	0.164***
	(0.063)	(0.087)	(0.042)
Wind *u*	0.161	0.146	0.135*
	(0.083)	(0.108)	(0.059)
Wind *v*	0.077	0.09	0.109
	(0.079)	(0.105)	(0.061)
Wind Speed	0.612***	0.671***	0.119
	(0.135)	(0.178)	(0.097)
IWV	0.687***	0.82***	0.235***
	(0.088)	(0.117)	(0.062)
IVT	0.124	-0.016	0.207**
	(0.116)	(0.15)	(0.078)
Soil	0.418***	0.477***	0.264***
	(0.105)	(0.139)	(0.079)
Snow	0.54***	0.621***	0.069
	(0.099)	(0.127)	(0.07)
Adjusted R-Squared	0.4278		0.2997
AIC		1081.4	

* $p < 0.05$, ** $p < 0.01$, *** $p < 0.001$

Table 3.6 Reduction of model to parsimonious model

Variable	Model1	Model2	Model3	Model4	Model5	Model6
Intercept	2.283***	2.283***	2.283***	2.283***	2.283***	2.283***
	(0.071)	(0.069)	(0.068)	(0.061)	(0.059)	(0.059)
Policies	0.906***				0.568***	0.562***
	(0.071)				(0.061)	(0.061)
IVT		1.097***			0.842***	
		(0.069)			(0.061)	
Soil			1.153***		0.928***	
			(0.068)		(0.061)	
IVT * Soil				1.512***		1.372***
				(0.061)		(0.061)
Adjusted R Squared	0.1272	0.1872	0.2069	0.3566	0.3899	0.4023

* p < 0.05, ** p < 0.01, *** p < 0.001

Table 3.7 Parsimonious model results

Variable	Model1	Model2	Model3
Intercept	2.283***	-0.043	4.495***
	(0.059)	(0.074)	(0.048)
Policies	0.562***	0.623***	0.152***
	(0.061)	(0.079)	(0.041)
IVT * Soil	1.372***	1.388***	0.524***
	(0.061)	(0.101)	(0.04)
Adjusted R-Squared	0.4023		0.2732
AIC		1126.2	

* $p < 0.05$, ** $p < 0.01$, *** $p < 0.001$

As described in Table 3.5, in our initial set of models we find the number of policies in the affected area to have a positive effect and to be highly significant. Wind speed and IWV are the most significant of the AR intensity variables, both with positive effects. Coefficients on the zonal and meridional components are both positive, indicating a positive effect of wind flow from the southeast to the northwest, though these effects are not significant. IVT has a positive effect in the simple loss model and a very slightly negative effect in the model of the logit model. Neither of these effects are significant. This is likely because IWV and wind speed already capture the effect of IVT. Antecedent soil moisture and snowpack both have positive and significant effects in the simple loss model and in the model of the log odds of positive losses.

The signs of the coefficients and the significance levels are remarkably similar for the simple loss model and the logit model. This is unsurprising since the average occurrence of loss (positive damages versus no damages) forms a large component of the average total magnitude of loss. Minor differences emerge when looking at the second stage of the nested model, modeling the logarithm of losses conditional on losses being positive. Policies are still significant with positive effect. The zonal and meridional components of wind remain positive with the zonal component gaining significance at the 5% level. The effect of IWV remains positive and significant. IVT gains a positive and significant effect at the 1% level. Wind speed drops out as a significant predictor, probably displaced by IVT and the zonal component of wind speed. Soil moisture remains a positive and significant predictor, while snow depth drops out of the model.

The overall adjusted R^2 for the simple model is 0.4278, indicating that the simple model captures 42.78% of the variance. This is somewhat higher than expected, given the large number of events with zero damages, and the low frequency of highly damaging events. The Akaike

Information Criterion (AIC) of the logit model is 1081.4 (*c.f.* 1126.2 in the parsimonious model, below). The adjusted R^2 for the second stage log linear model of the nested model is 0.2997. This again is somewhat higher than expected; it is lower than the percent of variance explained in the simple model because the first stage of the nested model has already accounted for a large proportion of the overall variance, and because the sample size is effectively half of that in the simple model.

In Table 3.6 we consider individually the effects of the number of policies, the intensity of the AR event as measured by IVT, the effect of antecedent soil moisture, and the combined effect of IVT and antecedent soil moisture. The best performing model is that which contains the number of policies in the affected area and the interaction between IVT and antecedent soil moisture. This model accounts for 40.23 percent of the variance, slightly less than the 42.78 percent captured in the full model presented in Table 3.5. The effects of policies and the interaction of IVT and soil moisture are both positive and highly significant ($p < 0.001$). Examining each component in isolation we find that the number of policies alone accounts for roughly 13% of the variance, IVT accounts for 19% of the variance, soil moisture accounts for 21% of the variance, and the interaction term of IVT with soil moisture accounts for 36% of the variance. Hence, of all the regressors considered, the simplest regressor with relatively good performance is the interaction of IVT with soil moisture. We note that these are log-linear models hence the effect of IVT and soil moisture on losses is nonlinear, or exponential. These effects are explored further in Figure 3.9 below.

The final selected parsimonious models are presented in Table 3.7. The simple model captures 40.23% of the variance with positive and highly significant effects of the number of

policies in affected areas and the interaction of IVT with antecedent soil moisture. Compare this to the full model which captures 42.78 percent of the variance. In the nested model, the effects of the number of policies and the interaction between IVT and soil moisture are positive and strongly significant in both the first and second stage of the model. AIC is slightly higher in the parsimonious model (1126.2 versus 1081.4) indicating slightly worse fit in the parsimonious model, as expected, and the adjusted R^2 in the second-stage log-linear model of losses conditional on losses being positive is 0.2732, slightly lower than the 0.2997 in the full model. Overall these are strong models considering the nature of the AR event data in which over half of all events result in zero damages, and a very small number of large events accounts for a very large proportion of total damages. Again we stress that these are log-linear models. We considered a wide range of non-linear specifications. The log-linear models generally outperformed models with other non-linear specifications and were simpler and easier to interpret.

Further model results are listed in the Appendix where we report model results for each initial crossing latitude. By and large the results are consistent with the models reported above. In some models a better fit is achieved by including maximum wind speed and IWV in place of IVT, which makes sense from a conceptual standpoint because integrated vapor transport consolidates the components of zonal and meridional air flow and the integrated water vapor levels. In several location-specific models the number of policies did not affect the model fit. This is not surprising since almost all of the variation in the number of policies is between locations, not within given locations.

At 30N the meridional *v* component of wind is significant, at 35 both *u* and *v* components are significant, and at 42.5 and 47.5N, the zonal *u* component is significant. This fits with the

orientation analysis above. Also in some areas initial snow depth provided slightly better model fit than antecedent soil moisture, and vice versa. There was no clear north-south pattern to these differences.

Figure 3.9 presents a visual depiction of the main regression results above. In these figures we plot IVT and antecedent soil moisture exceedances. We break IVT and soil moisture into deciles. For each decile we calculate the mean of losses given that IVT or soil moisture levels are equal to or above that decile, and the fraction of events that cause damages. We observe that estimated probabilities of loss increase from 40 to 80 percent as IVT increases from zeroth to ninetieth percentile. This increase is almost linear. The probability of loss associated with increases in antecedent soil moisture increase from 40 to 90 percent, again in a nearly linear fashion. Mean insured losses increase from below $1m to over $4m per event. The increase is roughly exponential. Mean losses increase in a similar fashion with antecedent soil moisture.

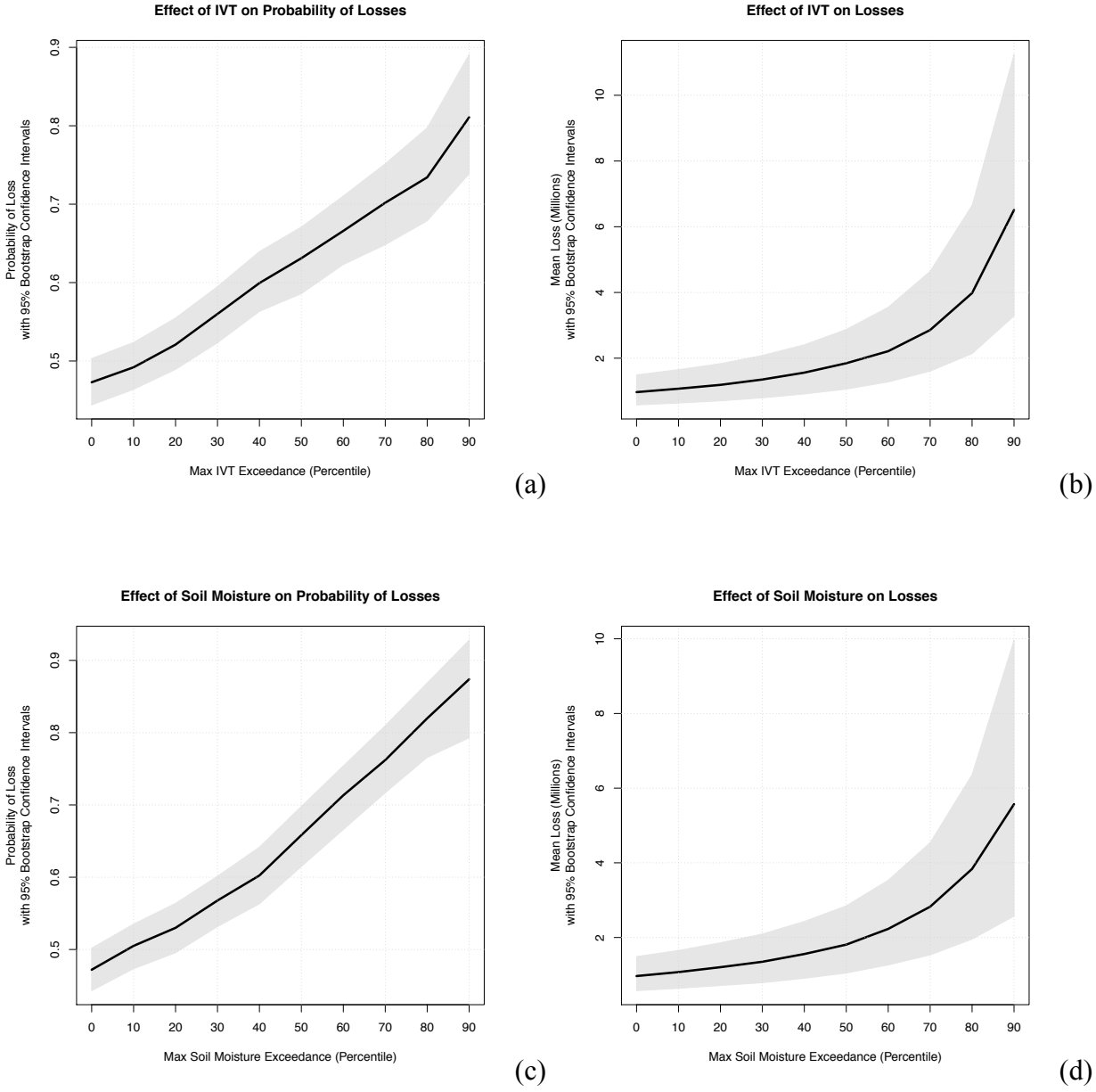

Figure 3.9: Probability and loss by IVT exceedances and antecedent soil moisture. (a) mean frequency of positive loss by AR event, increasing from 48% for all observations to 82% for observations with IVT over its 90th percentile; (b) mean loss in millions USD increasing as IVT exceeds its 0th to 90th percentiles. (c-d) are analogous figures plotting frequency of positive loss and mean loss against event soil moisture exceedances. 95% confidence intervals were bootstrapped with 1000 replicates.

4 Conclusions

This is the first paper to quantify the economic effects of atmospheric rivers on flood damages. From a 30 year (1977-2007) record of ARs and NFIP data, we find that atmospheric rivers are the principal drivers of insured flood losses in the western United States; 48 percent of AR events cause insured losses. AR events cause average total estimated damages of $20m, and can cause damages in excess of $1b. The key drivers of losses are exposure to risk (number of policies, total coverage in force), intensity of AR event as measured by maximum IVT, and antecedent snow depth or soil moisture levels. Damages increase exponentially with the intensity of AR events, and have the greatest impacts when land surface hydrology is already primed for flooding.

The spatial and temporal characteristics of flood damages closely follow the underlying hydro-climatology, after controlling for exposure to risk. Our results are in line with previous event-based studies which have found damages on the order of $1.5b for extreme events (Perry 2005), with damages driven by rain on snow events or by multiple AR events in succession.

Over the thirty year time sample there are only 24 days, comprising 13 separate events, on which insured losses exceed $10m, estimated to cause over $300m in total economic impacts. These 24 days account for 53.1 percent of total insured losses; only one occurred in the absence of AR conditions on the day of or the day preceding damages. It is clear that understanding these extreme events is the key to understanding flood damages in the western US.

Virtually all extreme flood loss events are caused by atmospheric rivers. Over our sample period AR events dominated flood losses from Washington to southern California with substantial

impacts also occurring in interior western states. ARs making landfall at a given latitude along the west coast often produce damage regionally from that latitude northward, owing to the breadth of ARs and the southwest to northeast orientation of many AR events.

Modeling results indicate that increased intensity of AR events as measured by IVT or IWV combined with wind speed produces increased damages, controlling for exposure to risk as measured by the number of policies in the affected area. The buildup of soil moisture from antecedent precipitation leads to greater damages from a given AR event controlling for AR intensity and exposure to risk. ARs often persist for 2 to 7 days and peak damages tend to occur the day after AR landfall.

As a result of anthropogenic climate change and the warming of the north Pacific Ocean, ARs are expected to become more frequent and more intense (Lavers *et al*. 2015, Gershunov *et al*., in preparation). This study shows that damages will increase nonlinearly with increases in intensity. The increase in exposure to risk over the next century, as population in the western coastal states continues to grow, is likely to drive losses even higher. On the other hand, snowpack in California, which contributes to damages, is expected to decrease by one half over the next century (Das *et al.* 2013). Depending on the timing and frequency of storms, this could have a dampening effect on losses.

This paper highlights the importance of spatially and temporally consistent data on flood damages. Just as physical monitoring networks have improved our understanding of the hydro-climatology of the western US, so must economic flood monitoring networks be improved to allow us to accurately quantify the competing influences changing exposure, intensification of storm events, and loss of snow pack in the coastal mountain ranges identified in this paper. Finally, this

work applies a large body of research that has shown the significance of atmospheric rivers in all aspects of west coast hydrology. We find that the dominant influence of ARs in causing hydrologic flooding translates directly to economic impacts. ARs are responsible for most of the significant flood events in the western US. Research into these phenomena is invaluable to understanding, mitigating, and responding to highly damaging flood events, that are expected to become more severe over the next century.

Acknowledgements

Chapter 3, in full, is currently being prepared for submission for publication of the material. Corringham, Thomas W.; Gershunov, Alexander; Cayan, Daniel R. Tom Corringham was the primary investigator and author of this material.

References

Nancy A. Barth, Gabriele Villarini, Munir A. Nayak, and Kathleen White. Mixed populations and annual flood frequency estimates in the western united states: The role of atmospheric rivers. Water Resources Research, 53(1):257–269, 2016.

California Department of Water Resources. California's flood future California's flood future: Recommendations for managing the state's flood risk. Technical report, DWR, November 2013.

Stanley A. Changnon, Roger A. Pielke Jr., David Changnon, Richard T. Sylves, and Roger Pulwarty. Human factors explain the increased losses from weather and climate extremes. Bulletin of the American Meteorological Society, 81(3):437–442, 2000.

Stanley D. Changnon. Measures of economic impacts of weather extremes. Bulletin of the American Meteorological Society, 84(9):1231–1235, 2003.

Tapash Das, Edwin P. Maurer , David W. Pierce , Michael D. Dettinger , and Daniel R. Cayan. Increases in flood magnitudes in California under warming climates. Journal of Hydrology, 501: 101–110, 2013.

Michael Dettinger. Climate change, atmospheric rivers, and floods in california – a multimodel analysis of storm frequency and magnitude changes. JAWRA Journal of the American Water Resources Association, 47(3):514–523, 2011.

Michael D. Dettinger. Sturm und drang—California's remarkable storm-drought connection. Hydrolink, pages 21–22, May 2015.

Michael D. Dettinger, Fred Martin Ralph, Tapash Das, Paul J. Neiman, and Daniel R. Cayan. Atmospheric rivers, floods and the water resources of california. Water, 3(2):445–478, 2011.

E. García-Bustamante, J. F. González-Rouco, J. Navarro, E. Xoplaki, P. A. Jiménez, and J. P. Montávez. North Atlantic atmospheric circulation and surface wind in the Northeast of the Iberian Peninsula: uncertainty and long term downscaled variability. Climate Dynamics, 38(1-2):141–160, January 2012.

Alexander Gershunov and Tim P. Barnett. Interdecadal modulation of enso teleconnections. Bulletin of the American Meteorological Society, 79(12):2715–2725, 1998.

Alexander Gershunov and Daniel R. Cayan. Heavy daily precipitation frequency over the contiguous United States: Sources of climatic variability and seasonal predictability. Journal of Climate, 16(16):2752–2765, 2003.

Alexander Gershunov, Tamara Shulgina, F. Martin Ralph, David A. Lavers, and Jonathan J. Rutz. Assessing the climate-scale variability of atmospheric rivers affecting western North America. Geophysical Research Letters, 44(15):7900–7908, 2017. 2017GL074175.

Diane P. Horn and Jared T. Brown. Introduction to the National Flood Insurance Program (NFIP). Technical report, Congressional Research Service, November 2017.

William G. Hoyt and Walter B. Langbein. Floods. Princeton University Press, 1955.

Dale Kasler, Ryan Sabalow, Peter Hecht, and Bill Lindelof. Northern California digs out, as another 'atmospheric river' takes shape. Sacramento Bee, January 13, 2017.

Howard O. Kunreuther. Introduction. In Howard O. Kunreuther and Richard J. Roth, Sr., editors, Paying the Price: The Status and Role of Insurance Against Natural Disasters in the United States, pages 1–16. Joseph Henry Press, Washington D.C., 1998.

Xu Liang, Dennis P. Lettenmaier, Eric F. Wood, and Stephen J. Burges. A simple hydrologically based model of land surface water and energy fluxes for general circulation models. Journal of Geophysical Research: Atmospheres, 99(D7):14415–14428, 1994.

Erwann O. Michel-Kerjan. Catastrophe economics: The national flood insurance program. Journal of Economic Perspectives, 24(4):165–86, December 2010.

Paul J. Neiman, F. Martin Ralph, Benjamin J. Moore, Mimi Hughes, Kelly M. Mahoney, Jason M. Cordeira, and Michael D. Dettinger. The landfall and inland penetration of a flood-producing atmospheric river in Arizona. Part I: Observed synoptic-scale, orographic, and hydrometeorological characteristics. Journal of Hydrometeorology, 14(2):460–484, 2013.

Paul J. Neiman, Lawrence J. Schick, F. Martin Ralph, Mimi Hughes, and Gary A. Wick. Flooding in western washington: The connection to atmospheric rivers. Journal of Hydrometeorology, 12(6):1337– 1358, 2011.

Edward T. Pasterick. The National Flood Insurance Program. In Howard O. Kunreuther, editor, Paying the Price: The Status and Role of Insurance Against Natural Disasters in the United States, pages 125–154. Joseph Henry Press, Washington D.C., 1998.

Charles A. Perry. Summary of significant floods in the United States and Puerto Rico, 1994 through 1998 water years. Scientific Investigations Report 2005–5194, U.S. Geological Survey, 2005.

Roger A. Pielke Jr. and Mary W. Downton. Precipitation and damaging floods: Trends in the United States, 1932–97. Journal of Climate, 13(20):3625–3637, 2000.

Roger A. Pielke, Jr., Mary W. Downton, and J. Zoe Barnard Miller. Flood damage in the United States, 1926–2000 a reanalysis of National Weather Service estimates. Technical report, Environmental and Societal Impacts Group National Center for Atmospheric Research, 2002.

Keith Porter, Anne Wein, Charles Alpers, Allan Baez, Patrick Barnard, James Carter, Alessandra Corsi, James Costner, Dale Cox, Tapash Das, Michael Dettinger, James Done, Charles Eadie, Marcia Eymann, Justin Ferris, Prasad Gunturi, Mimi Hughes, Robert Jarrett, Laurie Johnson, Hanh Dam Le-Griffin, David Mitchell, Suzette Morman, Paul Neiman, Anna Olsen, Suzanne Perry, Geoffrey Plumlee, Martin Ralph, David Reynolds, Adam Rose, Kathleen Schaefer, Julie Serakos, William Siembieda, Jonathon Stock, David Strong, Ian Sue Wing, Alex Tang, Pete Thomas, Ken Topping, Chris Wills, Lucile Jones, and Dale Cox. Overview of the ARkStorm scenario. Technical Report Open-File Report 2010-1312, U.S. Geological Survey, 2010.

F. M. Ralph and M. D. Dettinger. Storms, floods, and the science of atmospheric rivers. Eos, Transactions American Geophysical Union, 92(32):265–266, 2011.

F. Martin Ralph, Paul J. Neiman, Gary A. Wick, Seth I. Gutman, Michael D. Dettinger, Daniel R. Cayan, and Allen B. White. Flooding on california's russian river: Role of atmospheric rivers. Geophysical Research Letters, 33(13), 2006.

Jonathan J. Rutz, W. James Steenburgh, and F. Martin Ralph. Climatological characteristics of atmospheric rivers and their inland penetration over the western United States. Monthly Weather Review, 142(2):905–921, 2014.

Yong Zhu and Reginald E. Newell. A proposed algorithm for moisture fluxes from atmospheric rivers. Monthly Weather Review, 126(3):725–735, 1998.

Appendix

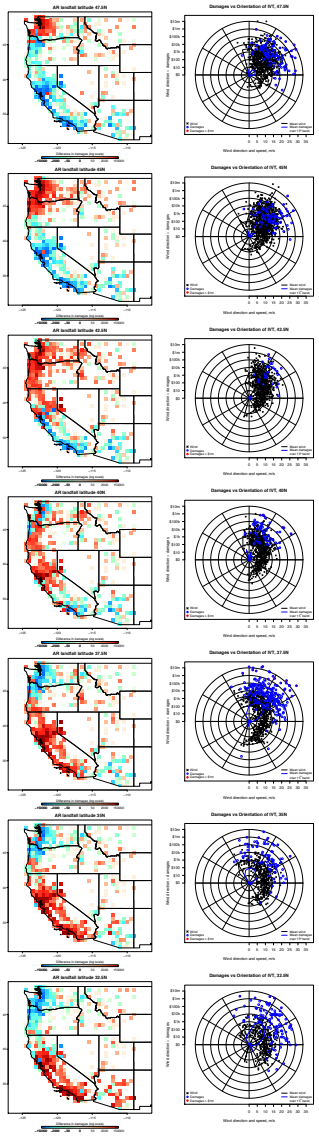

Figure 3.10 Full set of spatial composites and orientation of AR wind field

Table 3.8 Regression results by latitude band.

Latitude	27.5N	30N	32.5N	35N	37.5N	40N	42.5N	45N	47.5N
Intercept	-5.41874*	-11.6970	2.5462	-7.2858	-15.5681***	-8.1227***	-19.0669***	-3.3502***	-10.3252***
	(2.19166)	(6.0399)	(1.6269)	(3.5782)	(2.8386)	(1.6176)	(2.8901)	(0.8233)	(1.7053)
Policies								0.00001495***	0.00001059***
								(0.00000354)	(0.00000258)
Max IVT							0.0088***		
							(0.0024)		
Max IWV	0.08435*	0.1992		0.2654**	0.1605*		0.3621***		0.1699***
	(0.03985)	(0.1155)		(0.0952)	(0.0772)		(0.0935)		(0.0532)
Max Wind Speed	0.63020***				0.5415***	0.5896***			0.2103***
	(0.11170)				(0.0966)	(0.0886)			(0.0563)
Zonal Wind u				0.6303**			0.3210		0.1972***
				(0.2037)			(0.1718)		(0.0744)
Meridional Wind v		0.2799		0.2575					
		(0.1808)		(0.1301)					
Snow Depth		18.7574**			16.0505***		15.1015***		
		(5.9012)			(3.1547)		(3.0062)		
Soil Moisture				6.4539*		8.1839***			5.9539***
				(2.8936)		(2.1886)			(1.0981)
IVT * Snow								0.02355***	
								(0.0027)	
IVT * Soil			0.0177***						
			(0.0044)						
Degrees of Freedom	138	41	27	29	117	111	105	171	333
Adjusted R2	0.1817	0.2226	0.3514	0.5261	0.4738	0.4609	0.5035	0.3918	0.3723

* $p < 0.05$, ** $p < 0.01$, *** $p < 0.001$

Here we provide a description of the methodology used to create AR event data for regression analysis, including figures depicting the links between latitude bands and affected counties: In an prior auxiliary analysis, for each AR crossing latitude, over all dates in our sample, we recorded the counties with daily log losses significantly correlated with maximum IVT at that latitude on that day using a log linear model ($\log \text{loss}_{it} = \alpha + \beta\ \text{IVT}_{it}$) for each county and latitude. The threshold for significant effect was set at $p < 0.001$ on the coefficient estimate. Maps of affected counties by AR landfall latitude obtained using this methodology are presented in Figure 3.11.

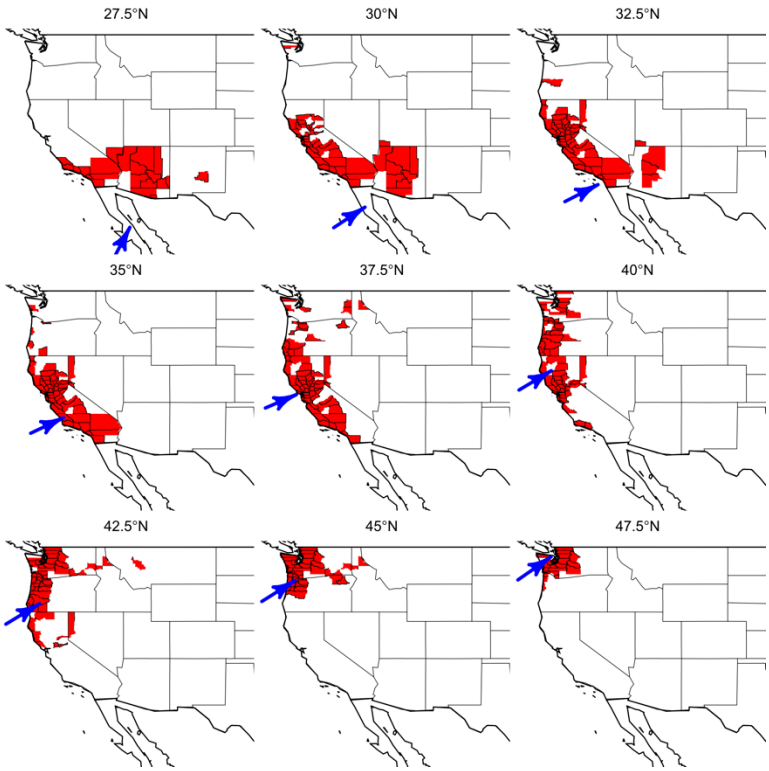

Figure 3.11: Affected counties associated with AR landfall at nine latitude bands.

For each event we then listed all counties associated with the active crossing latitudes during that particular event, using the lists of associated counties obtained in the auxiliary analysis.

Next, for each event, to capture the economic impact of the event, we aggregated the total number of claims, claims paid, and losses over significantly associated counties over the course of the event (1 to 14 days). To capture total vulnerability or exposure associated with each event, we recorded the total number of policies in force, the total coverage, and total premium payments for that policy year, over the associated counties at the first day of the event.

We included several variables to capture the intensity of the AR event, including maximum IVT, IWV, and wind speed over active crossing latitudes over the duration of the event, and variables to capture the directionality of the event, including mean *u* and *v* components of IVT.

Using VIC hydrology data we calculated the total antecedent soil moisture aggregated over the associated counties for the full set of crossing latitudes observed during the event. Antecedent moisture was calculated at 1 to 3 days preceding the start date of the event. We conducted sensitivity analyses varying the measure of antecedent moisture levels (soil moisture at different depths, snowpack, *etc.*) and the time lead. We present results of the analysis with the strongest overall effect of antecedent conditions. We also included month of year, and year to capture seasonal effects and time trends. We interacted month of year and year with initial crossing latitude to capture heterogeneous seasonal and secular time effects.

Other variables we could have included but did not include antecedent river flow, as measured by Hydro-Climatic Data Network gauges located in associated counties, water-year-to-date precipitation. Whether these or other hydrologic measures would yield better fitting models in describing and predicting the effects of AR events, and flood damages more generally, remains an open question and could form the focus for future research.